

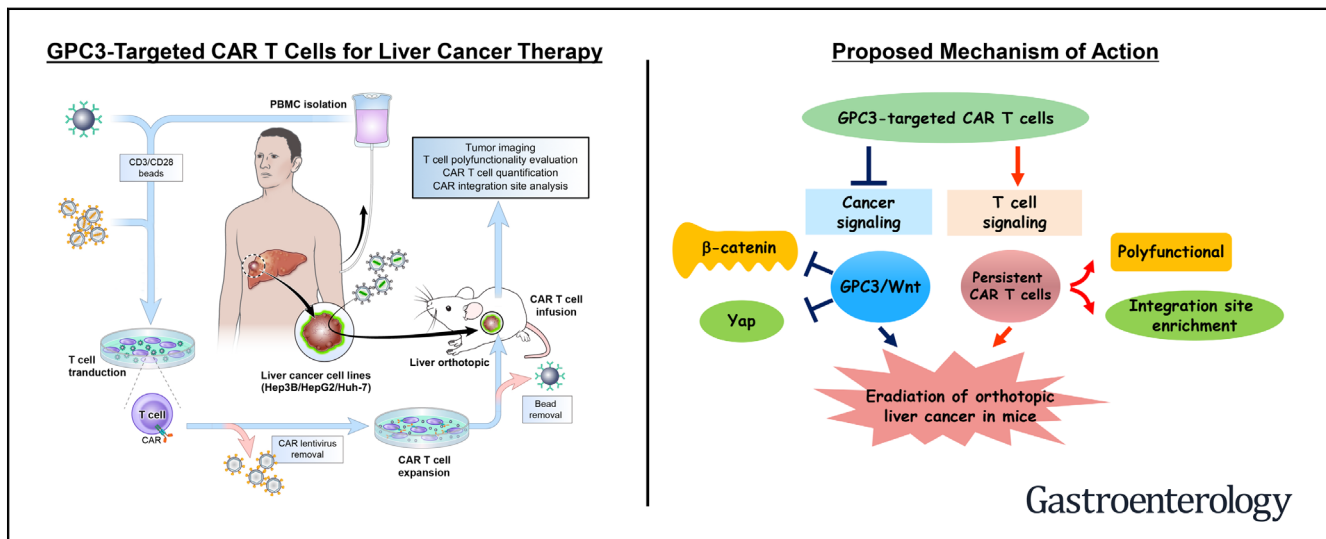
# BASIC AND TRANSLATIONAL—LIVER

## Persistent Polyfunctional Chimeric Antigen Receptor T Cells That Target Glypican 3 Eliminate Orthotopic Hepatocellular Carcinomas in Mice



Dan Li,<sup>1,2,\*</sup> Nan Li,<sup>1,\*</sup> Yi-Fan Zhang,<sup>1</sup> Haiying Fu,<sup>1,3</sup> Mingqian Feng,<sup>1</sup> Dina Schneider,<sup>4</sup> Ling Su,<sup>5</sup> Xiaolin Wu,<sup>5</sup> Jing Zhou,<sup>6</sup> Sean Mackay,<sup>6</sup> Josh Kramer,<sup>7</sup> Zhijian Duan,<sup>1</sup> Hongjia Yang,<sup>1</sup> Aarti Kolluri,<sup>1</sup> Alissa M. Hummer,<sup>1</sup> Madeline B. Torres,<sup>1</sup> Hu Zhu,<sup>8</sup> Matthew D. Hall,<sup>8</sup> Xiaoling Luo,<sup>9</sup> Jinqui Chen,<sup>9</sup> Qun Wang,<sup>2</sup> Daniel Abate-Daga,<sup>10</sup> Boro Dropulic,<sup>4</sup> Stephen M. Hewitt,<sup>11</sup> Rimas J. Orentas,<sup>12</sup> Tim F. Greten,<sup>13</sup> and Mitchell Ho<sup>1</sup>

<sup>1</sup>Laboratory of Molecular Biology, Center for Cancer Research, National Cancer Institute, National Institutes of Health, Bethesda, Maryland; <sup>2</sup>School of Life Sciences, East China Normal University, Shanghai, China; <sup>3</sup>Department of Immunology, Norman Bethune College of Medicine, Jilin University, Changchun, China; <sup>4</sup>Lentingen, a Miltenyi Biotec Company, Gaithersburg, Maryland; <sup>5</sup>Cancer Research Technology Program, Leidos Biomedical Research, Inc, Frederick, Maryland; <sup>6</sup>IsoPlexis Corporation, Branford, Connecticut; <sup>7</sup>Animal Facility, Leidos Biomedical Research, Inc, National Cancer Institute, National Institutes of Health, Bethesda, Maryland; <sup>8</sup>Chemical Genomics Center, National Center for Advancing Translational Sciences, National Institutes of Health, Rockville, Maryland; <sup>9</sup>Collaborative Protein Technology Resource, National Cancer Institute, National Institutes of Health, Bethesda, Maryland; <sup>10</sup>Departments of Immunology, Cutaneous Oncology, and Gastrointestinal Oncology, H. Lee Moffitt Cancer Center and Research Institute, Tampa, Florida; <sup>11</sup>Laboratory of Pathology, Center for Cancer Research, National Cancer Institute, National Institutes of Health, Bethesda, Maryland; <sup>12</sup>Seattle Children's Research Institute, Seattle, Washington; and <sup>13</sup>Thoracic and Gastrointestinal Oncology Branch, Center for Cancer Research, National Cancer Institute, National Institutes of Health, Bethesda, Maryland



**BACKGROUND AND AIMS:** Glypican 3 (GPC3) is an oncofetal antigen involved in Wnt-dependent cell proliferation that is highly expressed in hepatocellular carcinoma (HCC). We investigated whether the functions of chimeric antigen receptors (CARs) that target GPC3 are affected by their antibody-binding properties. **METHODS:** We collected peripheral blood mononuclear cells from healthy donors and patients with HCC and used them to create CAR T cells, based on the humanized YP7 (hYP7) and HN3 antibodies, which have high affinities for the C-lobe and N-lobe of GPC3, respectively. NOD/SCID/IL-2R $\gamma$ C $^{null}$  (NSG) mice were given intraperitoneal injections of luciferase-expressing (Luc) Hep3B or HepG2 cells and after xenograft tumors formed, mice were given injections of saline

or untransduced T cells (mock control), or CAR (HN3) T cells or CAR (hYP7) T cells. In other NOD/SCID/IL-2R $\gamma$ C $^{null}$  (NSG) mice, HepG2-Luc or Hep3B-Luc cells were injected into liver, and after orthotopic tumors formed, mice were given 1 injection of CAR (hYP7) T cells or CD19 CAR T cells (control). We developed droplet digital polymerase chain reaction and genome sequencing methods to analyze persistent CAR T cells in mice. **RESULTS:** Injections of CAR (hYP7) T cells eliminated tumors in 66% of mice by week 3, whereas CAR (HN3) T cells did not reduce tumor burden. Mice given CAR (hYP7) T cells remained tumor free after re-challenge with additional Hep3B cells. The CAR T cells induced perforin- and granzyme-mediated apoptosis and reduced levels of active  $\beta$ -catenin in HCC cells.

Mice injected with CAR (hYP7) T cells had persistent expansion of T cells and subsets of polyfunctional CAR T cells via antigen-induced selection. These T cells were observed in the tumor microenvironment and spleen for up to 7 weeks after CAR T-cell administration. Integration sites in pre-infusion CAR (HN3) and CAR (hYP7) T cells were randomly distributed, whereas integration into *NUP1L1* was detected in 3.9% of CAR (hYP7) T cells 5 weeks after injection into tumor-bearing mice and 18.1% of CAR (hYP7) T cells at week 7. There was no common site of integration in CAR (HN3) or CD19 CAR T cells from tumor-bearing mice. **CONCLUSIONS:** In mice with xenograft or orthotopic liver tumors, CAR (hYP7) T cells eliminate GPC3-positive HCC cells, possibly by inducing perforin- and granzyme-mediated apoptosis or reducing Wnt signaling in tumor cells. GPC3-targeted CAR T cells might be developed for treatment of patients with HCC.

**Keywords:** Hepatic; Immunotherapy; Tumor-Specific T Cells; Lymphocyte.

Robust efficacy of chimeric antigen receptor (CAR) T cells targeting CD19 in B-cell malignancies has led to the approval of 2 CD19 CAR T-cell products by the US Food and Drug Administration.<sup>1,2</sup> However, the translation of CAR T cells for solid tumors remains an unmet challenge. Glycan 3 (GPC3) is a glycosylphosphatidylinositol-anchored cell surface protein consisting of a core protein and 2 heparan sulfate chains.<sup>3</sup> GPC3 is an oncofetal protein expressed in >70% of hepatocellular carcinoma (HCC)<sup>4,5</sup> and other solid tumors, including hepatoblastoma and lung squamous cell carcinoma.<sup>6,7</sup> Its expression is not detected in nonmalignant adult tissues, including normal liver.<sup>6,8</sup> Mechanistically, GPC3 can promote tumor growth by modulating the Wnt/Frizzled signaling complex on HCC cells.<sup>9–11</sup> Various antibody-based therapies, including immunotoxins,<sup>12,13</sup> antibody-drug conjugates,<sup>14</sup> CAR T cells or bispecific antibodies targeting GPC3<sup>15–21</sup> have been developed. Recent evidence indicated that CAR T cells targeting GPC3 could inhibit the growth of HCC cells.<sup>15,16,18</sup> Preliminary results showed a modest response with GPC3-targeted CAR T cells in a phase 1 trial of 13 patients in China.<sup>22</sup> To improve its anti-tumor activity, their research group is modifying the CAR construct via co-expressing a soluble PD-1 protein.<sup>21</sup>

Considerable progress has been made in improving the signaling domains of CARs. However, another challenge in developing effective CAR T-cell therapy is the functional optimization of antibody domains. We hypothesize that the function of CARs is affected by their epitope specificity, affinity, and functional activity. In the present study, we used the antibodies HN3<sup>23</sup> and humanized YP7 (hYP7)<sup>24,25</sup> with comparable high affinity for the N-lobe and C-lobe of GPC3, respectively, to engineer CAR T cells and evaluated their antitumor properties. We developed the methods to analyze tissue persistence and genomic integration sites of the CAR T cells.

## WHAT YOU NEED TO KNOW

### BACKGROUND AND CONTEXT

Glycan 3 (GPC3) is an oncofetal antigen that promotes Wnt-dependent cell proliferation and is highly expressed in hepatocellular carcinoma (HCC). Chimeric antigen receptors (CARs) that target GPC3 are in development for treatment of HCC.

### NEW FINDINGS

In mice with xenograft or orthotopic liver tumors, GPC3-targeted CAR T cells reduced Wnt signaling in HCC cells and caused tumor regression.

### LIMITATIONS

This study was performed in mice; studies are needed in humans.

### IMPACT

GPC3-targeted CAR T cells might be developed for treatment of patients with HCC.

## Methods

### Generation of Glycan 3–Targeted Chimeric Antigen Receptor T Cells

The antigen recognition region from the HN3 (pMH288), hYP7 (pMH289), and the anti-CD19 antibody FMC63 (pMH376) was subcloned into the second-generation (2G) CAR construct, which contains expressing cassettes encoding the CD8α hinge and transmembrane region, a 4-1BB costimulatory domain, the intracellular CD3ζ, the self-cleaving T2A sequence, and the truncated human epidermal growth factor receptor for cell tracking and ablation. The truncated human epidermal growth factor receptor lacks the domains essential for ligand binding and tyrosine kinase activity, but it retains the binding epitope of anti-EGFR monoclonal antibody cetuximab.<sup>26</sup> A third-generation (3G) CAR (hYP7) construct containing both 4-1BB and CD28 costimulatory domains was also made. The CAR T cells were produced as described previously.<sup>27</sup>

### Animal Studies

Five-week-old female NOD/SCID/IL-2R $\gamma$ null (NSG) mice (National Cancer Institute, Frederick, MD) were housed and treated under the protocol (LMB-059) approved by the Institutional Animal Care and Use Committee at the National Institutes of Health. For the peritoneal Hep3B model, 3 million luciferase-expressing Hep3B (Hep3B-Luc) cells were intraperitoneally (IP) injected into mice. Mice with established tumors were then randomly allocated into 6 groups and IP infused

\* Authors share co-first authorship.

**Abbreviations used in this paper:** CAR, chimeric antigen receptor; ddPCR, droplet digital polymerase chain reaction; 2G, second generation; 3G, third generation; GPC3, glycan 3; HCC, hepatocellular carcinoma; hYP7, humanized YP7; IP, intraperitoneal; IV, intravenous; Luc, luciferase-expressing; NSG, NOD/SCID/IL-2R $\gamma$ null; PSI, polyfunctional strength index.

 Most current article

© 2020 by the AGA Institute  
0016-5085/\$36.00

<https://doi.org/10.1053/j.gastro.2020.02.011>

once with varying conditions as follows: saline only (phosphate-buffered saline); 5 million untransduced T cells (mock); 5 million CAR (HN3) T cells; 5 million CAR (hYP7) T cells; 10 million CAR (hYP7) T cells; and 20 million CAR (hYP7) T cells. For the peritoneal HepG2 model, 2 million HepG2-Luc cells were IP injected into male mice. Mice with established tumors were randomly allocated into 2 groups and IP infused once with mock T cells or CAR (hYP7) T cells. For the orthotopic HepG2 or Hep3B model, mice were inoculated with 0.5 million HepG2-Luc or Hep3B-Luc tumor cells in the liver. After 2 or 3 weeks of tumor establishment, mice were intravenously (IV) infused once with CAR (hYP7) T cells. The CD19 CAR T cells were used as control. For the Hep3B re-challenge model, 4 weeks after CAR (hYP7) T-cell administration, mice were re-challenged with 0.5 million Hep3B-Luc tumor cells (IP) and followed for 2 weeks. Tumors were measured by total bioluminescent flux using a Xenogen IVIS Lumina (PerkinElmer, Waltham, MA).

### Droplet Digital Polymerase Chain Reaction

Genomic DNA from cells was isolated using the FlexiGene DNA kit (Qiagen, Hilden, Germany). Droplet digital polymerase chain reaction (ddPCR) experiments were performed on a QX200 ddPCR system (Bio-Rad, Hercules, CA) according to the manufacturer's instructions. CAR vector-specific primers and probe were multiplexed with either a human (MKL2) or mouse (Tfrc) reference gene assay. The primers and probes sequences were listed in *Supplementary Material*.

### Integration Site Analysis

CAR lentivector integration site analysis was performed using linker-mediated PCR adapted from a procedure described previously for measuring viral infection in patients with human immunodeficiency virus.<sup>28</sup> Briefly, sample DNA is randomly sheared, end-repaired, and ligated to a linker. The integration site is amplified with 1 primer specific to the lentivector LTR and another primer specific to the linker. The amplified product is subjected to high-throughput Illumina Sequencing (Illumina, San Diego, CA). Integration sites in the sample are identified and quantified for further analysis. The primer sequences designed for the present study are listed in *Supplementary Material*. The raw data for all CAR integration sites identified in the present study are provided as *Supplementary Data Sheets 1–3*.

## Results

### Chimeric Antigen Receptor (Humanized YP7) T Cells Are More Potent Than Chimeric Antigen Receptor (HN3) T Cells

To evaluate the effect of GPC3 epitopes in CAR T-cell killing, we compared the HN3<sup>23</sup> and hYP7<sup>24,25</sup> antibodies that recognizes the N-lobe and C-lobe of GPC3, respectively (Figure 1A). The HN3<sup>13</sup> and YP7 antibodies are highly tumor-specific for their binding on tumor cells and tissues (*Supplementary Figure 1–4*). To produce CAR T cells for testing in HCC cell and animal models (Figure 1B), the antigen recognition region of the HN3 or the hYP7 antibody was cloned into lentiviral vectors encoding either the 2G

CAR with 4-1BB costimulatory domain or the 3G CAR with 4-1BB and CD28 costimulatory domains (Figure 1C). The expression of CARs in transduced T cells was detected through recombinant GPC3 protein staining and cell surface truncated human epidermal growth factor receptor expression (*Supplementary Figure 5*). In view of potential off-target toxicity induced by the 3G CAR (hYP7) T cells (*Supplementary Figure 6A*), the 2G CAR construct was used for the rest of our study unless otherwise noted.

Next, we evaluated the expansion of GPC3-targeted CAR T cells from healthy donors and HCC patients (*Supplementary Figure 6B*). After expansion, CAR (hYP7) T cells derived from healthy donors were composed of similar ratios of CD4<sup>+</sup> and CD8<sup>+</sup> T-cell subsets (Figure 1D). Interestingly, we observed substantial variations in the frequency of CD4<sup>+</sup> (43%–93%) and CD8<sup>+</sup> T cells (7%–57%) in HCC patients. We then compared the cytolytic capability of CAR (HN3) and CAR (hYP7) T cells in HCC cells. As shown in Figure 1E and F, CAR (hYP7) T cells displayed higher lytic activity than CAR (HN3) T cells in Hep3B cells. At the effector to target ratio of 5, lytic activity of HCC patient-derived CAR (hYP7) T cells ranged from 34% to 73%, with a mean of 54%, which was lower than the average activity (92%) of healthy donor-derived CAR (hYP7) T cells, possibly due to low CD8<sup>+</sup> T-cell number in HCC patients. Minimal cell lysis was observed in Hep3B cells treated with mock T cells (*Supplementary Figure 6C*) or the GPC3 knockout Hep3B cells treated with CAR (hYP7) T cells (*Supplementary Figure 6D*), demonstrating target-dependent specificity. Furthermore, additional liver cancer cell lines including HepG2 and Huh-7 were also lysed by CAR (HN3) and CAR (hYP7) T cells (*Supplementary Figure 6E and F*). CAR (hYP7) T cells were significantly more potent in eliminating HepG2 cells than CAR (HN3) T cells during the period of 140 hours (Figure 1G). In addition, CAR (hYP7) T cells produced more cytokines and chemokines than CAR (HN3) T cells in the presence of Hep3B or HepG2 cells (*Supplementary Figure 7*). Collectively, CAR (hYP7) T cells exhibit better cytolytic ability than CAR (HN3) T cells. CAR T cells derived from HCC patients are able to kill GPC3-positive HCC cells.

### Chimeric Antigen Receptor (Humanized YP7) T Cells Are Highly Polyfunctional

Polyfunctional T cells, a subset of T cells capable of co-producing 2 or more cytokines/chemokines at the single-cell level, are recently reported for their association with long-term immune responses in the clinical settings.<sup>29–31</sup> Here, we used the 32-plex panel that included the key immune elements of T cells (Figure 2A). The polyfunctional strength index (PSI) values are defined by cytokine function to highlight the contribution of each group to the overall polyfunctionality of the sample.<sup>29</sup> As shown in Figure 2B and C, CAR (hYP7) T cells from a healthy donor showed remarkably higher PSI than CAR (HN3) T cells when stimulated with Hep3B (11-fold) or G1 (77-fold) cells, whereas no increase of PSI was shown in CAR (hYP7) T cells stimulated by

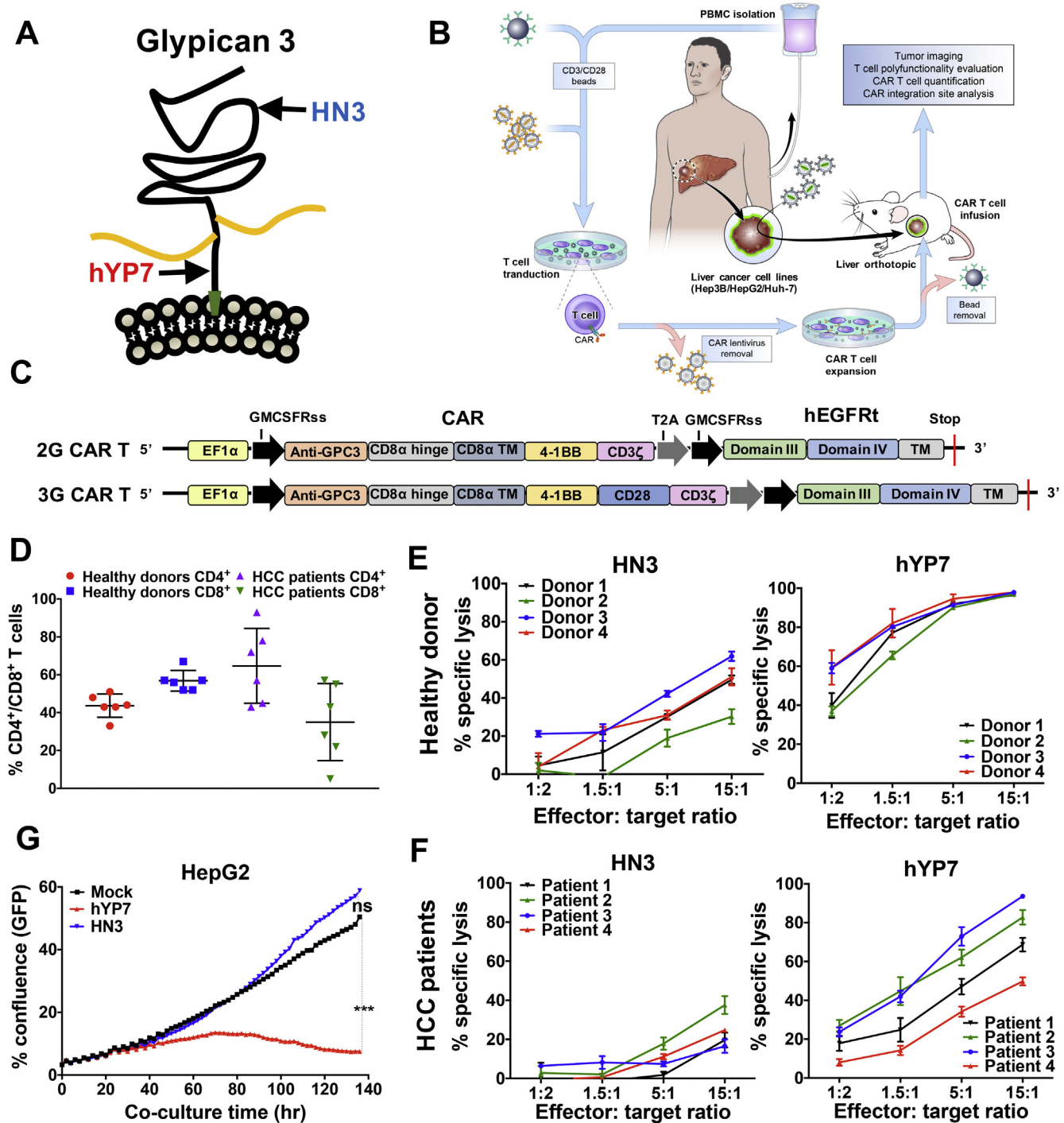


**Figure 1.** GPC3-targeted CAR T cells kill GPC3-positive HCC cells in vitro. (A) The binding of 2 antibodies to GPC3. HN3 binds to the N-lobe of GPC3 around residue 41 (phenylalanine). YP7 binds to the C-lobe of GPC3 (residue 521–530). (B) Schematic of CAR T-cell production and evaluation in mouse models. (C) Schematic of the 2G and 3G CAR constructs. (D) CD4<sup>+</sup> and CD8<sup>+</sup> T-cell analysis of CAR (hYP7) T cells from 6 healthy donors and 6 HCC patients. (E, F) Cytolytic activity of CAR (HN3) T cells and CAR (hYP7) T cells from healthy donors (E) and HCC patients (F) after 24 hours of co-culture with Hep3B cells. (G) GPC3-targeted CAR T-cell-mediated killing of HepG2 cells as determined by using IncuCyte zoom. HepG2 cells were incubated with CAR T cells at the effector to target ratio of 2:1 up to 140 hours. GFP, green fluorescent protein; hEGFRt, truncated human epidermal growth factor receptor. Values represent mean  $\pm$  SEM. \*\*\* $P$  < .001; ns, not significant.

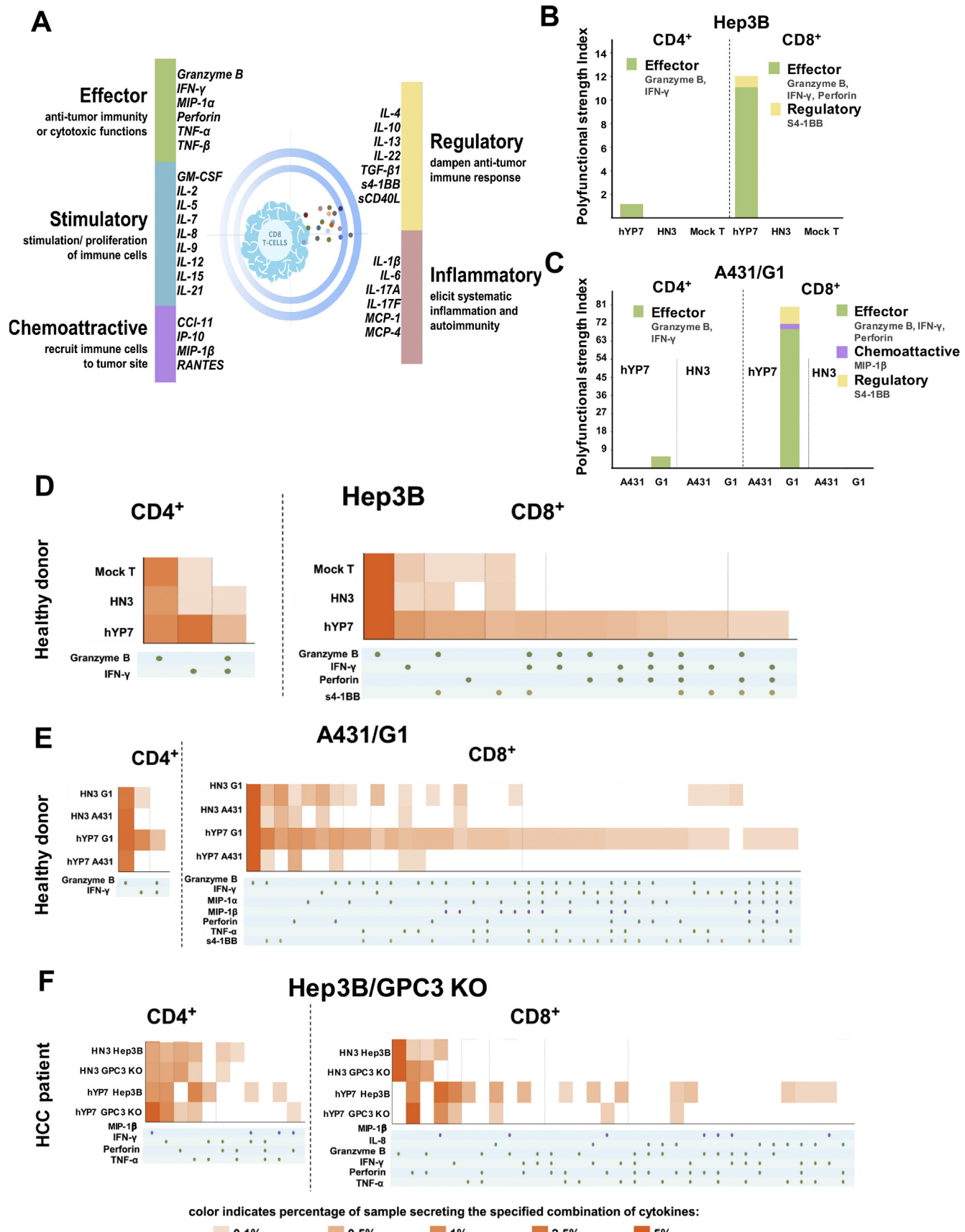
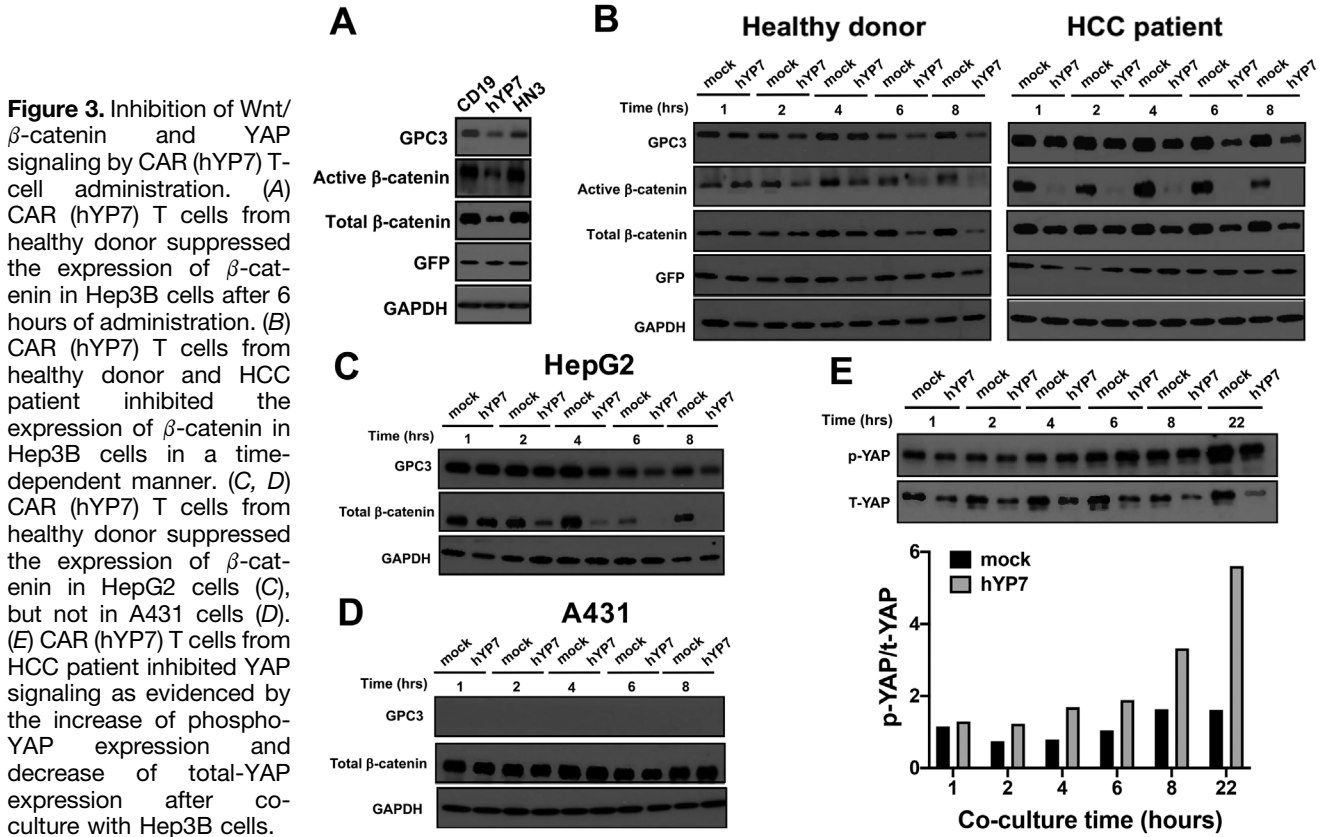


**Figure 2.** Cytokine/chemokine profiles of polyfunctionality of T cells redirected with GPC3. (A) The validated 32-plex panel including 5 groups of cytokines: effector, stimulatory, chemoattractive, regulator, and inflammatory. (B, C) PSI computed for



antigen-negative A431 (Figure 2C). Moreover, CD8<sup>+</sup> CAR (hYP7) T PSI is 8 and 11 times higher than CD4<sup>+</sup> CAR (hYP7) T PSI when cocultured with Hep3B and G1 cells, respectively, indicating CD8<sup>+</sup> CAR T cells were more polyfunctional than CD4<sup>+</sup> CAR T cells. To distinguish the polyfunctional subsets within each sample, we used a polyfunctional heatmap visualization to display major secreted functional subsets. As shown in Figure 2D, a 4-plex group containing granzyme B, interferon gamma, perforin, and s4-1BB was only expressed by a small subset of CD8<sup>+</sup> CAR (hYP7) T cells upon Hep3B stimulation. The G1-stimulated CD8<sup>+</sup> CAR (hYP7) T cells were more polyfunctional with a small subset secreting a 7-plex group containing granzyme B, interferon gamma, CCL-3, CCL-4, perforin, TNF-α, and s4-1BB (Figure 2E).

We also examined the polyfunctionality of CAR T cells from an HCC patient (no. 3, Supplementary Table 1) after stimulated with Hep3B cells. Consistent with polyfunctional profiles of healthy donor-derived CAR T cells, the pronounced up-regulation of polyfunctional groups was only found in CAR (hYP7) product, predominantly in CD8<sup>+</sup> T cells, but not in CAR (HN3) product from the HCC patient

(Figure 2F). Interestingly, the HCC patient-derived polyfunctional CD8<sup>+</sup> CAR (hYP7) T cells were not only composed of effector cytokines (granzyme B, interferon gamma, and perforin), but also additional cytokines/chemokines (TNF-α, MIP-1β, and interleukin 8) that were not secreted by CD8<sup>+</sup> CAR (hYP7) T cells from the healthy donor (Figure 2D). Taken together, CAR (hYP7) derived from both the healthy donor and the HCC patient stimulated robust activation and expansion of polyfunctional T cells, particularly through small subsets of CD8<sup>+</sup> cytotoxic T cells, which lyse tumor cells by inducing perforin/granzyme apoptosis pathway.

#### Chimeric Antigen Receptor T Cells Targeting Glycan 3 Inhibit Wnt Signaling in Hepatocellular Carcinoma

Previous studies have shown that GPC3 interacts with Wnt ligands and promotes HCC cell proliferation by facilitating Wnt/Frizzled binding.<sup>9–12</sup> To determine whether GPC3-targeted CAR T cells affected Wnt signaling in HCC cells, we measured active and total β-catenin levels. CAR

←  
healthy donor-derived GPC3-targeted CAR T cells co-cultured with Hep3B (B) and G1/A431 (C) cells for 20 hours at the single-cell level. (D, E) Polyfunctional heatmap displaying major functional cytokines/chemokines secreted across GPC3-specific CAR T cells from healthy donor upon Hep3B (D) and G1/A431 (E) cell stimulation. (F) Polyfunctional heatmap of HCC patient-derived GPC3-specific CAR T cells upon Hep3B and GPC3 knockout Hep3B cell stimulation for 20 hours.

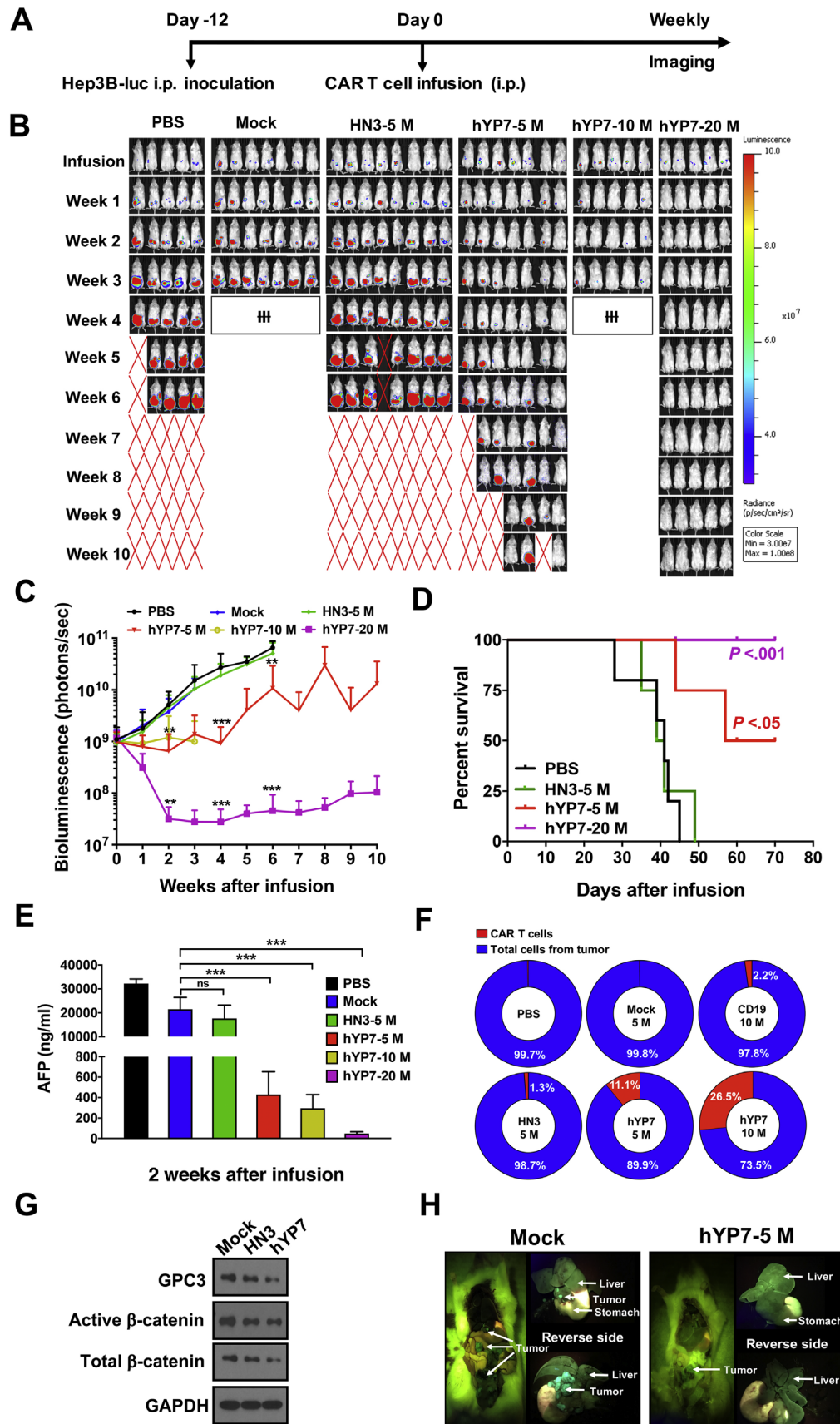


**Figure 4.** CAR (hYP7) T cells eradicate tumors in the peritoneal Hep3B xenograft mouse model. (A) Experimental schematic. Hep3B tumor-bearing NSG mice were intraperitoneal (i.p.) injected with mock T cells (mock), 5 million CAR (HN3) T cells (HN3-5M), and 5, 10, and 20 million CAR (hYP7) T cells (hYP7-5M, hYP7-10M, hYP7-20M). (B) CAR (hYP7) T cells regressed established Hep3B xenografts at high dose (20M) and inhibited tumor growth at low doses (5M and 10M), whereas CAR (HN3) T cells did not inhibit tumor growth. Symbol “#” indicated that mice were euthanized in advance for analysis. (C) Tumor bioluminescence in mice treated in Figure 4B. (D) Kaplan-Meier survival curve of mice after infusion. (E) α-Fetoprotein (AFP) levels in serum collected from groups shown in Figure 4B after 2 weeks of injection. (F) Detection of CAR vector-positive cells in xenograft tumor tissues after 3 weeks of injection. (G) CAR (hYP7) T cells caused the reduction of active- and total-β-catenin levels as compared with mock T-cell-treated mice. (H) Representative pictures of mouse from mock and hYP7-10M group. PBS, phosphate-buffered saline. Values represent mean  $\pm$  SEM. \* $P < .05$ ; \*\* $P < .01$ ; \*\*\* $P < .001$ ; ns, not significant.

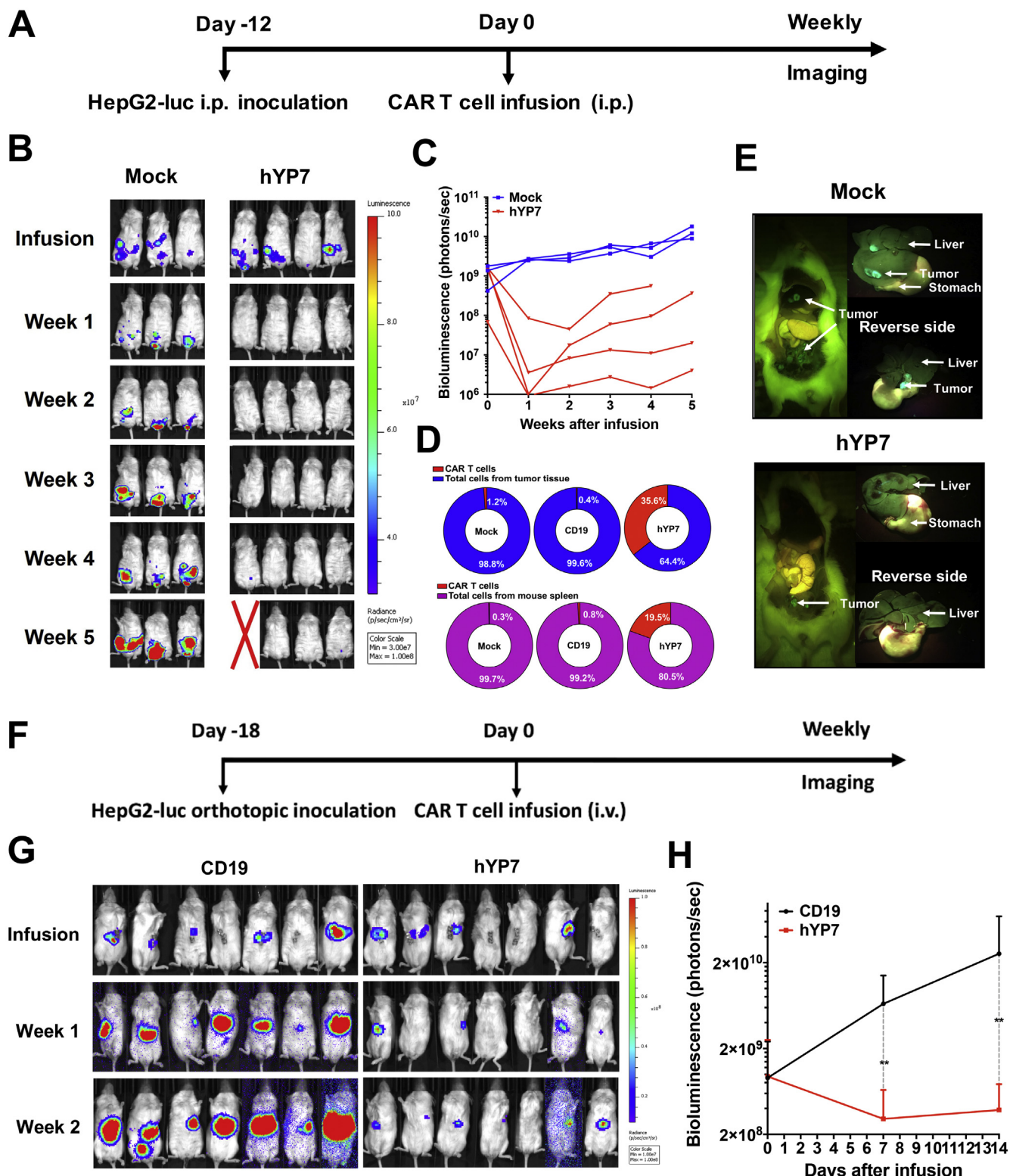
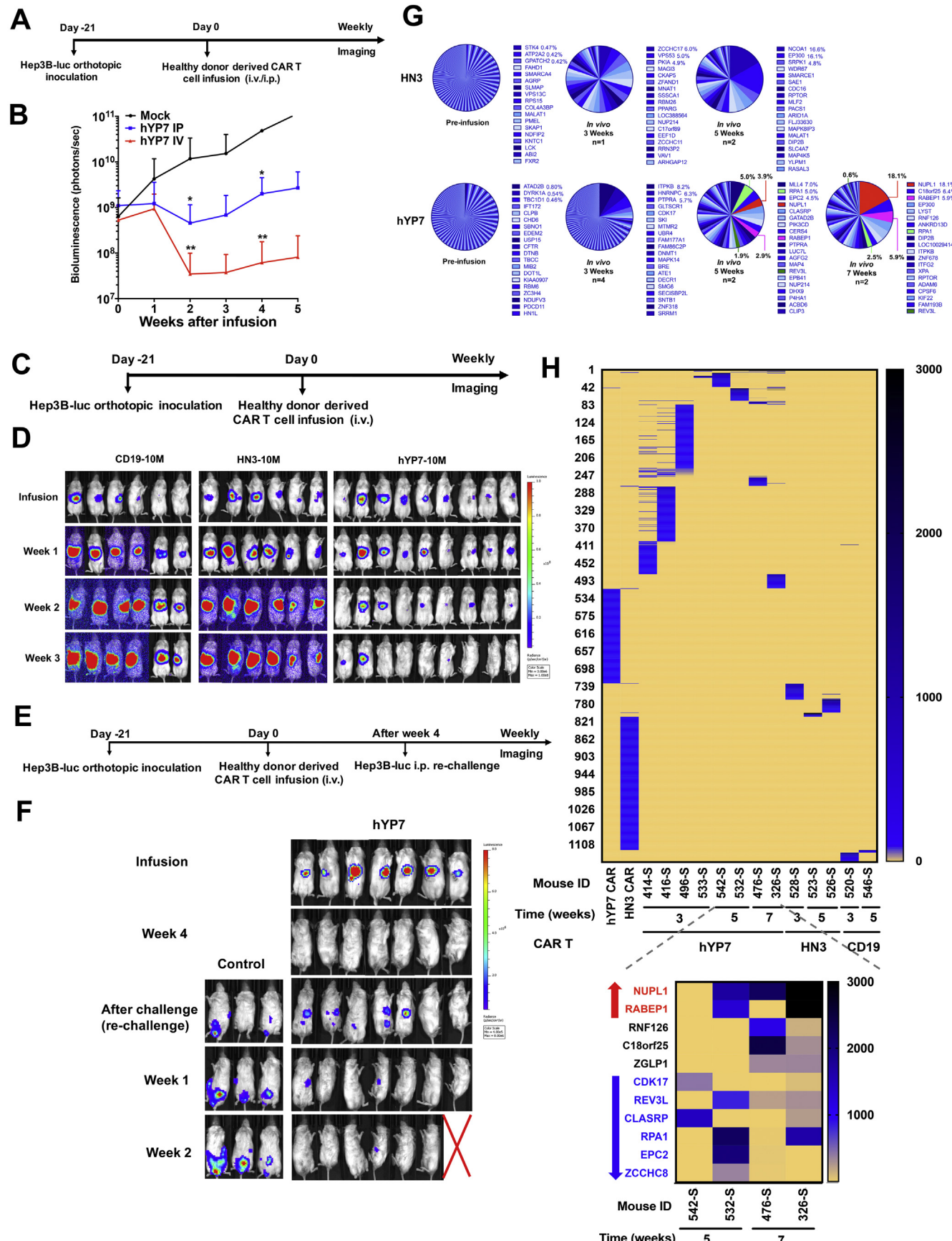


**Figure 5.** CAR (hYP7) T cells eliminate tumor cells in the HepG2 xenograft mouse models. (A) Experimental schematic of the peritoneal HepG2 xenograft mouse model. HepG2 tumor-bearing male NSG mice were intraperitoneal (i.p.) injected with 20 million mock T cells or CAR (hYP7) T cells. (B) CAR (hYP7) T cells demonstrated potent antitumor activity and mediated eradication of HepG2 xenograft tumors. (C) Tumor bioluminescence in mice treated in Figure 5B. (D) Detection of CAR vector-positive cells in tumor and spleen from mice after 5 weeks of injection. (E) Representative pictures of mouse from mock and hYP7 groups. (F) Experimental schematic of the orthotopic HepG2 xenograft model. HepG2 tumor-bearing female NSG mice were infused with 10 million CD19 CAR T cells and CAR (hYP7) T cells. (G) CAR (hYP7) T cells regressed growth of orthotopic HepG2 tumors. (H) Tumor bioluminescence in mice treated in Figure 5G. Values represent mean  $\pm$  SEM. \*\* $P$  < .01.



(hYP7) T cells from a healthy donor significantly reduced the expression of active  $\beta$ -catenin and total  $\beta$ -catenin after co-cultured with Hep3B cells, while CAR (HN3) T cells and CD19 CAR T cells failed to inhibit  $\beta$ -catenin expression (Figure 3A). Interestingly, we found that CAR (hYP7) T cells from the HCC patient no. 3 dramatically suppressed the expression of active  $\beta$ -catenin to a greater extent than the healthy donor-derived CAR (hYP7) T cells (Figure 3B). In addition, CAR (hYP7) T cells were able to inhibit  $\beta$ -catenin expression in HepG2 cells (Figure 3C), but not GPC3-negative A431 cells (Figure 3D). Furthermore, previous reports have shown that GPC3 regulates the expression of YAP, a key effector molecule in the Hippo pathway in HCC.<sup>23,32</sup> Here, we observed the increased phosphorylated YAP and reduced total YAP expression in Hep3B cells treated with CAR (hYP7) T cells from the HCC patient (Figure 3E). Together, our results indicate that targeting GPC3 by CAR (hYP7) T cells can suppress the Wnt/ $\beta$ -catenin and Yap signaling in HCC cells.

### *Chimeric Antigen Receptor (Humanized YP7) T Cells Suppress the Growth of Hepatocellular Carcinoma Xenografts in Mice*

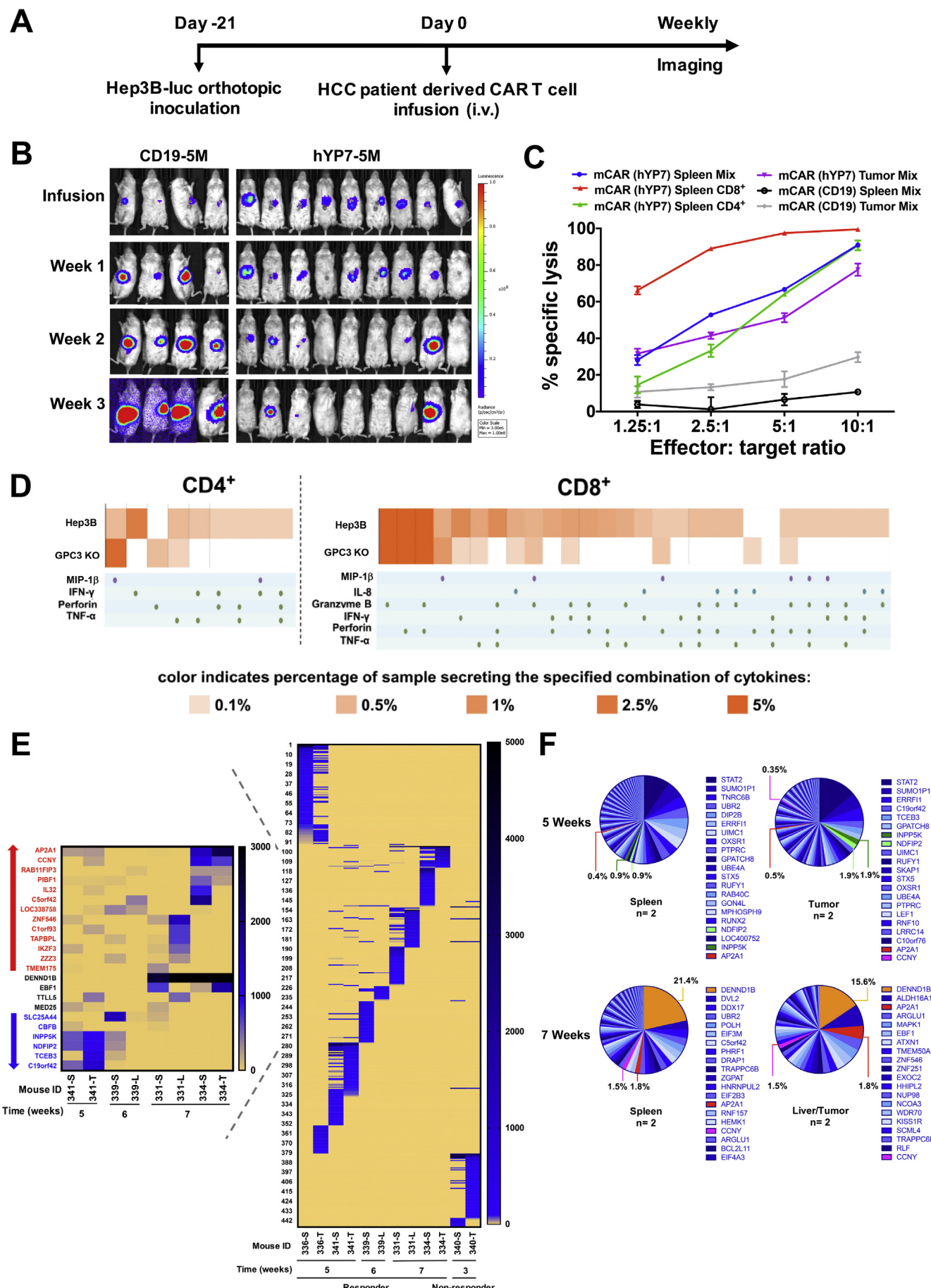
To evaluate the antitumor activities of GPC3-specific CAR T cells in vivo, NSG female mice were intraperitoneally (IP) injected with Hep3B-Luc cells (Figure 4A). Various doses of CAR (hYP7) T cells all showed reduced tumor burden compared with the mock group (Figure 4B and C). No significant tumor growth inhibition was seen in the mice treated with CAR (HN3) T cells. Mice receiving 20 million CAR (hYP7) T cells were all alive without recurrence by day 70, compared with 50% survival in the 5 million CAR (hYP7) T-cell group (Figure 4D). Although GPC3-targeted CAR T cells initially caused a loss in body weight, mice gradually regained weight (Supplementary Figure 8). Moreover, the serum  $\alpha$ -fetoprotein (AFP) levels in mice treated with 5 million (mean, 429 ng/mL) or 10 million (mean, 296 ng/mL) CAR (hYP7) T cells were significantly lower than the levels in mock T cell-treated mice (mean, 21,467 ng/mL) after 2 weeks of administration (Figure 4E). Notably, the  $\alpha$ -fetoprotein levels in mice treated with 20 million CAR (hYP7) T cells were in the range of 25–78 ng/mL, which is close to the cutoff value (20 ng/mL) in human adults.<sup>33</sup> Robust in vivo expansion

and survival of genetically modified T cells are considered critical predictors of durable clinical remissions in cancer patients. We assessed the percentage of CAR T cells using ddPCR, which allows measurement of absolute gene copy number to determine CAR vector-positive cells. As shown in Figure 4F, 10.1% of cells were CAR vector-positive in the 5 million CAR (hYP7) group, whereas only 1.3% of cells were CAR vector-positive in the 5 million CAR (HN3) group after 3 weeks of administration. In the 10 million CAR (hYP7) group, 26.5% of CAR vector-positive cells were detected, demonstrating an inverse correlation between tumor burden and T-cell persistence over time.

Consistent with the inhibitory effect of silencing GPC3 on Wnt signaling in vitro, CAR (hYP7) T-cell administration down-regulated active and total  $\beta$ -catenin levels compared with the mock group in vivo (Figure 4G). From the peritoneal Hep3B xenograft mouse model, we found that mice developed tumor lesions on the liver and other organs within the abdominal cavity (Figure 4H). Interestingly, Hep3B tumors in the mice treated with 5 million CAR (hYP7) T cells grew locally and were restricted to the adipose tissue away from the mouse liver, suggesting that a low dose of CAR (hYP7) T cells can prevent tumors from seeding and growing in the liver as well as spreading to other organs.

A previous report showed that HCC tumors grew faster and had a higher volume in male than female NSG mice,<sup>34</sup> which highlights the need for using male mice in liver cancer studies. To evaluate the efficacy of CAR (hYP7) T cells in another liver cancer xenograft mouse model, we IP inoculated HepG2 cells into male NSG mice (Figure 5A). Encouragingly, CAR (hYP7) T cells were able to regress tumor growth (Figure 5B and C), indicating that efficacy of GPC3-targeted CAR T cells is sex-independent. After 5 weeks of CAR (hYP7) T-cell administration, ddPCR detected 35.6% and 19.5% of CAR vector-positive cells from tumor and mouse spleen, respectively (Figure 5D). By contrast, we did not detect CAR vector-positive cells in either tissue from CD19 CAR T cell-treated mouse. Furthermore, we found that human HepG2 cells migrated to the mouse liver and CAR (hYP7) T cells restricted the liver metastasis of tumor cells (Figure 5E), which was similar to our observation in the peritoneal Hep3B xenograft mouse model.

**Figure 6.** Tumor eradication in the orthotopic Hep3B xenograft mouse model by CAR (hYP7) T cells from a healthy donor. (A) Experimental schematic. The orthotopic Hep3B tumor-bearing NSG mice were IP or IV injected with 20 million CAR (hYP7) T cells. (B) Mice treated with CAR (hYP7) T cells via tail vein (hYP7 IV) demonstrated tumor eradication, while intraperitoneal infusion (hYP7 IP) resulted in tumor growth inhibition. (C) Experimental schematic. The orthotopic Hep3B tumor-bearing NSG mice were IV injected with 10 million CD19 CAR, CAR (HN3) and CAR (hYP7) T cells. (D) CAR (hYP7) T-cell administration regressed Hep3B tumor growth in mice, while CAR (HN3) T cells failed to inhibit tumor growth. (E) Experimental schematic of Hep3B tumor re-challenge. CAR (hYP7) –treated mice that showed no detectable tumor were IP implanted with 0.5 million Hep3B cells. As control, naïve mice were implanted with Hep3B cells following an injection of mock T cells. (F) CAR (hYP7)-treated mice resisted Hep3B tumor re-challenge. (G) Frequency of integrated genes in spleen (S) of mice treated with CAR (HN3) and CAR (hYP7) T cells at 3 weeks, 5 weeks, and 7 weeks post-infusion. The top 20 genes were listed. (H) Distribution of integration sites in spleen of mice treated with CD19 CAR, CAR (HN3), and CAR (hYP7) T cells over 3–7 weeks. The shared integrated genes in mice after 5–7 weeks of CAR (hYP7) T-cell injection was highlighted in a separate heatmap. Values represent mean  $\pm$  SEM. \* $P < .05$ ; \*\* $P < .01$ .



## Chimeric Antigen Receptor (Humanized YP7) T Cells Cause Tumor Regression in Orthotopic Xenograft Models

We further examined antitumor activity of CAR (hYP7) T cells in an orthotopic HCC mouse model. Hep3B-Luc cells were injected into the liver of NSG mice, healthy donor derived-CAR (hYP7) T cells were IP or IV infused 21 days after tumor inoculation (Figure 6A). Although both routes of administration of CAR (hYP7) T cells led to a reduction in tumor size and suppressed tumor growth compared to the control group, IV injection of CAR T cells (hYP7 IV) resulted in greater tumor regression than IP injection of CAR T cells (hYP7 IP) (Figure 6B), possibly because of preferred localization of CAR T cells to the liver via blood circulation.<sup>35</sup> At the end of this study, 75% of mice in the hYP7 IV group were tumor-free, whereas all mice in the mock group carried large tumors. Consistently, higher percentage of CAR vector-positive cells were detected in spleen and tumor microenvironment from the hYP7 IV group than tissues from the hYP7 IP group (Supplementary Figure 9). We also conducted toxicology analysis of CAR (hYP7) T cells by examining blood counts, serum chemistry and organ weights in mice (Supplementary Table 2).

Next, we compared the efficacy of healthy donor-derived CAR (HN3) and CAR (hYP7) T cells in the same orthotopic Hep3B xenograft mouse model (Figure 6C). As shown in Figure 6D, CAR (hYP7) T cells suppressed tumor growth and eliminated the tumor in 66% of mice by week 3, whereas CAR (HN3) T cells failed to reduce tumor burden. To determine the ability of persistent CAR (hYP7) T cells to prevent tumor relapse, mice that cleared initial tumor burden were re-challenged with Hep3B tumor cells (Figure 6E). While tumors grew rapidly in control mice, mice previously treated with CAR (hYP7) T cells remained tumor-free after Hep3B tumor re-challenge (Figure 6F). Moreover, efficacy of CAR (hYP7) T cells was also validated in another orthotopic (HepG2) xenograft mouse model (Figure 5F–H).

To analyze the molecular determinants of CAR (hYP7) T-cell efficacy and persistence, we analyzed the integration sites from the spleens of mice (showed in Figure 6D) treated with CAR (hYP7) T cells ( $n = 8$ ), CAR (HN3) ( $n = 3$ ), and CD19 CAR ( $n = 2$ ) from 3 to 7 weeks. As we expected, the integration sites from pre-infusion CAR (HN3) and CAR (hYP7) T cells were randomly distributed (Figure 6G). The integration into *NUPL1* was detected at a frequency of 3.9% 5 weeks after injection and increased to 18.1% at week 7,

whereas no integration site was shared and enriched in mice treated with CAR (HN3) T cells. Analysis of all the integration sites from each individual mouse identified 11 integration sites shared among different mice from 5 to 7 weeks (Figure 6H, Supplementary Table 3 and Supplementary Data Sheet 1). Some of these integration sites (eg, *NUPL1* and *RABEP1*) were enriched from 5 to 7 weeks, while some (eg, *REV3L* and *RPA1*) became diminished gradually. We also found largely different integration sites between a complete responder and a partial responder after 7 weeks of CAR (hYP7) T-cell injection (Supplementary Figure 10 and Supplementary Data Sheet 2). Interestingly, the 2 shared integration sites (*NUPL1* and *RABEP1*) decreased in the partial responder at week 7.

Finally, to evaluate the efficacy of CAR (hYP7) T cells derived from HCC patients, we again chose to use primary T cells isolated from the HCC patient no. 3, who was a 64-year-old male that had been treated with sorafenib for 6 months until his disease progressed. We produced CAR (hYP7) and CD19 CAR T cells from this HCC patient and used these cell products to treat mice engrafted orthotopically with Hep3B-Luc cells (Figure 7A). The patient-derived CAR (hYP7) T cells effectively eradicated Hep3B tumors in 77% of mice, whereas mice treated with CD19 CAR T cells succumbed to tumors 3 weeks post-T cell transfusion (Figure 7B). The same HCC patient-derived CAR (hYP7) T cells were able to eliminate Hep3B tumors in 75% of mice from a repeated experiment (Supplementary Figure 11). Furthermore, we characterized the function of persistent CAR (hYP7) T cells recovered from the spleen of treated mouse, named as mCAR (hYP7) T cells. As shown in Figure 7C, CD8<sup>+</sup> mCAR (hYP7) T cells exhibited significantly higher lytic activity than CD4<sup>+</sup> mCAR (hYP7) T cells against Hep3B cells. Furthermore, we found a profound increase of polyfunctionality in CD8<sup>+</sup> mCAR (hYP7) T cells (Figure 7D). The polyfunctional CAR T-cell subsets with combination of 3 or more cytokine secretions (MIP-1 $\beta$ , IL-8, granzyme B, interferon gamma, perforin, and TNF- $\alpha$ ) in both CD4<sup>+</sup> and CD8<sup>+</sup> T cells are largely increased only when cocultured with Hep3B cells but not with GPC3 knockout Hep3B cells, further demonstrating the specificity of CAR (hYP7) after *in vivo* passage.

We also analyzed the integration sites in mice treated with this HCC patient-derived CAR (hYP7) T cells from 3 to 7 weeks. As shown in Figure 7E, CAR (hYP7) showed a strong integration preference into distinct genes between responders and nonresponder. Notably, the integrated sites were largely shared between different tissues (eg, spleen

**Figure 7.** Persistent polyfunctional CAR (hYP7) T cells from a HCC patient eradicate orthotopic Hep3B xenograft tumors. (A) Experimental schematic. The orthotopic Hep3B tumor-bearing NSG mice were IV injected with 5 million CD19 CAR and CAR (hYP7) T cells. (B) CAR (hYP7) T cells regressed Hep3B tumor growth in mice. (C) CAR (hYP7) T cells recovered from mouse spleen after 4 weeks of injection named as mCAR (hYP7) T cells were cocultured with Hep3B cells, and cytolytic activity was analyzed 24 hours after coculture. (D) mCAR (hYP7) T cells showed profound increase of polyfunctionality by the stimulation of Hep3B cells, but not the GPC3 knockout Hep3B cells. (E) Distribution of integration sites in individual mouse treated with CAR (hYP7) T cells for 3–7 weeks. The shared integrated genes in mice after 5–7 weeks of CAR (hYP7) T-cell injection was highlighted in a separate heatmap. L, liver; S, spleen; T, tumor. (F) Frequency of integrated genes in spleen and liver/tumor of mice treated with CAR (hYP7) T cells from 5 weeks to 7 weeks post-infusion. The top 20 genes were listed. Values represent mean  $\pm$  SEM.

and liver) of the same mouse, indicating clonal expansion of CAR (hYP7) T cells in mice. Comparing with low abundance at 5 weeks post infusion, CAR (hYP7) integration into particular genes (eg, *AP2A1*, *CCNY*) were enriched at 7 weeks, while some integration events (eg, *INPP5K*, *NDFIP2*) became diminished at 7 weeks. The details of all 23 shared integrated genes can be found in *Supplementary Table 4* and *Supplementary Data Sheet 3*. Moreover, the CAR (hYP7) integration into *DENND1B* became the most dominant event at 7 weeks (spleen 21.4% and liver 15.6%) (*Figure 7F*). Taken together, we found that persistent CAR (hYP7) T cells had integration sites related to specific genes shared in different mice at different time points, indicating a potential selection pressure for integration sites in the genome for CAR T-cell activation, survival, and clonal expansion *in vivo*.

## Discussion

In the present study, we used the antibodies hYP7 and HN3 specifically for a membrane-proximal C-lobe epitope and a membrane-distal N-lobe epitope of GPC3 to make CAR T cells and analyzed their antitumor activities. The CAR (hYP7) T cells targeting the C-lobe of GPC3 close to the cell membrane showed superior antitumor activity by producing CAR T cells that not only induce perforin/granzyme-mediated apoptosis, but also inhibit Wnt/β-catenin signaling in tumor cells. We also used ddPCR and genomic sequencing methods to analyze the persistence of CAR T cells in mice and demonstrated a subset of the CAR (hYP7) T-cell clones that were enriched and expanded over 7 weeks after injection.

Various antibody-based therapeutic strategies including immunotoxins and antibody-drug conjugates targeting GPC3 have been developed for treating HCC.<sup>12–14</sup> The immunogenicity of immunotoxins and the likelihood of multidrug resistance to antibody-drug conjugate treatment are potential limitations for them to be used as single agents for reaching long-term tumor remission. An optimized GPC3-targeted CAR T-cell therapy for treating liver cancer may hold greater potential for achieving sustained tumor remission, despite the current challenge for treating solid tumors in general. The GPC3-targeted CAR T cells based on the GC33 antibody<sup>36</sup> have been made and are currently being tested for the treatment of HCC.<sup>15,18,22</sup> Although GC33 and YP7 are known to bind the C-lobe of GPC3, they recognize 2 distinct epitopes (*Supplementary Figure 12A*). Specifically, the GPC3 fragment (amino acid 521–530) is crucial for the binding ability of YP7, while GC33 does not bind to the same fragment. The CAR (hYP7) expressed on Jurkat T cells bind to GPC3 with higher affinity than GC33 CAR (*Supplementary Figure 12B*). We have compared 2G CAR (hYP7) and CAR (HN3) with the reported 3G CAR (GC33)<sup>15</sup> using the Huh-7 IP dissemination xenograft mouse model. We found that the CAR (hYP7) T cells reduced tumor burden more effectively than CAR (GC33) T cells (*Supplementary Figure 13*). It would be interesting to compare the efficacy and safety of CAR (hYP7) T-cell

therapy with CAR (GC33) T-cell therapy in future clinical studies.

Using single cell-based functional analysis, we found that the CD8<sup>+</sup> T cells showed a greater increase in polyfunctionality than CD4<sup>+</sup> T cells in CAR (hYP7) T cells from healthy donor and HCC patient. Moreover, HCC patient-derived CD8<sup>+</sup> CAR (hYP7) T cells recovered from mouse spleen showed a greater increase in percentages of polyfunctional T cells than the same patient-derived CD8<sup>+</sup> CAR (hYP7) T cells cultured *in vitro* by Hep3B stimulation (*Figures 2F* and *7D*). Future studies of evaluating HCC patient-derived CAR T cells in the same patient-derived xenograft model, as well as a murine HCC model<sup>37</sup> by hydrodynamic injection of oncogenes (eg, *MYC*) and *GPC3*, may further validate the efficacy of GPC3-targeted CAR T cells in the tumor microenvironment.

Membrane-proximal epitopes can facilitate efficient T-cell synapse formation,<sup>38,39</sup> which may explain the superior efficacy of CAR (hYP7) compared with CAR (HN3). In addition to its unique epitope specificity, the YP7 antibody may have the highest binding affinity among all known GPC3 antibodies, including GC33, which may also contribute to the potent efficacy of CAR (hYP7). Furthermore, CAR (hYP7) T cells have significantly higher polyfunctionality than CAR (HN3) T cells. Moreover, a subset of distinct integration sites in the T-cell genome are selected and enriched in different mice at different time points after a single injection of CAR (hYP7) T cells, not CAR (HN3) T cells. Taken together, differences in persistence, integration site preferences, and T-cell polyfunctionality may contribute to the discrepancy between efficacies of these 2 CAR constructs. Lastly, it has been shown that GPC3 may function as a co-receptor for Wnt and facilitate the Wnt/Frizzled signaling complex in HCC cells.<sup>9,10</sup> Wnt/β-catenin signaling is frequently up-regulated in HCC and is implicated in the maintenance of tumor-initiating cells, immune escape, and resistance.<sup>37,40</sup> We previously demonstrated that GPC3 affected Wnt/β-catenin signaling and that GPC3 knockout inhibited HCC tumor growth in cell and mouse models.<sup>11</sup> In the present study, we found significantly more reduction of GPC3 protein levels induced by the coculture with GPC3 (hYP7) CAR T cells than GPC3 (HN3) CAR T cells. More reduction of active β-catenin in HCC cells was also observed when cocultured with GPC3 (hYP7) CAR T cells than the GPC3 (HN3) CAR T cells. Surprisingly, hYP7 showed greater reduction in active β-catenin than HN3 in the CAR format, despite HN3 blocking the Wnt binding site on GPC3 as a naked antibody.<sup>11,12</sup> We speculate that the inhibition of Wnt/β-catenin signaling by GPC3-targeted CAR T cells is likely due to the decrease of GPC3 levels in HCC cells via an unknown mechanism rather than the impairment in the direct interaction between GPC3 and Wnt. Interestingly, it has been recently demonstrated that CAR T cells can provoke reversible antigen loss through the trogocytosis mechanism.<sup>41</sup> The reduction of Wnt signaling in tumor cells may further explain how CAR (hYP7) T cells could eradicate the HCC xenografts in mice.

Recent reports showed CAR T-cell-associated clonal expansion in a complete remission in patients with leukemia,<sup>42,43</sup> suggesting it is important to investigate candidate factors driving successful expansion in responders. In the present study, we analyzed the integration sites of CAR (hYP7) from a healthy donor and a HCC patient in mice. Many shared integrated genes were observed in different tissues on the same mouse, likely due to the expansion of selected clones. Several integration events (eg, *NUPL1*, *DENND1B*) have become highly abundant in multiple mice at weeks 5 and 7 after infusion. Interestingly, some of these integrations were located in the same orientation as the corresponding genes, which could lead to alternative splicing and affect their functions. *NUPL1* encodes a nucleoporin in the nuclear pore complex. Interestingly, deletion of *NUPL1* was found in some colorectal cancers and knockdown of *NUPL1* could promote cell growth.<sup>44</sup> Therefore, the insertion of CAR (hYP7) into *NUPL1* may potentially promote CAR T-cell growth. *DENND1B* plays an important role in regulating T-cell receptor internalization in T helper type 2 cells.<sup>45</sup> The clinical relevance of these integration sites remains unclear. Future studies analyzing persistent CAR T cells in HCC patients will validate shared integration sites ("hotspots") in the T-cell genome.

In conclusion, we have demonstrated that CAR (hYP7) T cells can induce sustained HCC tumor regression in mice as a GPC3-targeted CAR T-cell therapy that might be developed for treatment of patients with HCC.

## Supplementary Material

Note: To access the supplementary material accompanying this article, visit the online version of *Gastroenterology* at [www.gastrojournal.org](http://www.gastrojournal.org), and at <https://doi.org/10.1053/j.gastro.2020.02.011>.

## References

- Porter DL, Levine BL, Kalos M, et al. Chimeric antigen receptor-modified T cells in chronic lymphoid leukemia. *N Engl J Med* 2011;365:725–733.
- Kochenderfer JN, Dudley ME, Feldman SA, et al. B-cell depletion and remissions of malignancy along with cytokine-associated toxicity in a clinical trial of anti-CD19 chimeric-antigen-receptor-transduced T cells. *Blood* 2012;119:2709–2720.
- Filmus J, Shi W, Wong ZM, et al. Identification of a new membrane-bound heparan sulphate proteoglycan. *Biochem J* 1995;311(Pt 2):561–565.
- Hsu HC, Cheng W, Lai PL. Cloning and expression of a developmentally regulated transcript MXR7 in hepatocellular carcinoma: biological significance and temporal distribution. *Cancer Res* 1997;57:5179–5184.
- Capurro M, Wanless IR, Sherman M, et al. Glypican-3: a novel serum and histochemical marker for hepatocellular carcinoma. *Gastroenterology* 2003;125:89–97.
- Baumhoer D, Tornillo L, Stadlmann S, et al. Glypican 3 expression in human nonneoplastic, preneoplastic, and neoplastic tissues: a tissue microarray analysis of 4,387 tissue samples. *Am J Clin Pathol* 2008;129:899–906.
- Aviel-Ronen S, Lau SK, Pintilie M, et al. Glypican-3 is overexpressed in lung squamous cell carcinoma, but not in adenocarcinoma. *Mod Pathol* 2008;21:817–825.
- Montalbano M, Georgiadis J, Masterson AL, et al. Biology and function of glypican-3 as a candidate for early cancerous transformation of hepatocytes in hepatocellular carcinoma (review). *Oncol Rep* 2017;37:1291–1300.
- Capurro MI, Xiang YY, Lobe C, et al. Glypican-3 promotes the growth of hepatocellular carcinoma by stimulating canonical Wnt signaling. *Cancer Res* 2005;65:6245–6254.
- Gao W, Kim H, Feng M, et al. Inactivation of Wnt signaling by a human antibody that recognizes the heparan sulfate chains of glypican-3 for liver cancer therapy. *Hepatology* 2014;60:576–587.
- Li N, Wei L, Liu X, et al. A frizzled-like cysteine rich domain in glypican-3 mediates Wnt binding and regulates hepatocellular carcinoma tumor growth in mice. *Hepatology* 2019;70:1231–1245.
- Gao W, Tang Z, Zhang YF, et al. Immunotoxin targeting glypican-3 regresses liver cancer via dual inhibition of Wnt signalling and protein synthesis. *Nat Commun* 2015;6:6536.
- Fleming BD, Urban DJ, Hall M, et al. The engineered anti-GPC3 immunotoxin, HN3-ABD-T20, produces regression in mouse liver cancer xenografts via prolonged serum retention. *Hepatology* 2019 Sep 2014 [Epub ahead of print].
- Fu Y, Urban DJ, Nani RR, et al. Glypican-3-specific antibody drug conjugates targeting hepatocellular carcinoma. *Hepatology* 2019;70:563–576.
- Gao H, Li K, Tu H, et al. Development of T cells redirected to glypican-3 for the treatment of hepatocellular carcinoma. *Clin Cancer Res* 2014;20:6418–6428.
- Jiang Z, Jiang X, Chen S, et al. Anti-GPC3-CAR T cells suppress the growth of tumor cells in patient-derived xenografts of hepatocellular carcinoma. *Front Immunol* 2016;7:690.
- Ishiguro T, Sano Y, Komatsu SI, et al. An anti-glypican 3/CD3 bispecific T cell-redirection antibody for treatment of solid tumors. *Sci Transl Med* 2017;9.
- Li W, Guo L, Rathi P, et al. Redirecting T cells to glypican-3 with 4-1BB zeta chimeric antigen receptors results in Th1 polarization and potent antitumor activity. *Hum Gene Ther* 2017;28:437–448.
- Chen C, Li K, Jiang H, et al. Development of T cells carrying two complementary chimeric antigen receptors against glypican-3 and asialoglycoprotein receptor 1 for the treatment of hepatocellular carcinoma. *Cancer Immunol Immunother* 2017;66:475–489.
- Guo X, Jiang H, Shi B, et al. Disruption of PD-1 enhanced the anti-tumor activity of chimeric antigen receptor t cells against hepatocellular carcinoma. *Front Pharmacol* 2018;9:1118.
- Pan Z, Di S, Shi B, et al. Increased antitumor activities of glypican-3-specific chimeric antigen receptor-modified T

- cells by coexpression of a soluble PD1-CH3 fusion protein. *Cancer Immunol Immunother* 2018;67:1621–1634.
22. Zhai B, Shi D, Gao H, et al. A phase I study of anti-GPC3 chimeric antigen receptor modified T cells (GPC3 CAR-T) in Chinese patients with refractory or relapsed GPC3+ hepatocellular carcinoma (r/r GPC3+ HCC). *J Clin Oncol* 2017;35: 3049–3049.
  23. Feng M, Gao W, Wang R, et al. Therapeutically targeting glycan-3 via a conformation-specific single-domain antibody in hepatocellular carcinoma. *Proc Natl Acad Sci U S A* 2013;110:E1083–E1091.
  24. Phung Y, Gao W, Man YG, et al. High-affinity monoclonal antibodies to cell surface tumor antigen glycan-3 generated through a combination of peptide immunization and flow cytometry screening. *MAbs* 2012;4:592–599.
  25. Zhang YF, Ho M. Humanization of high-affinity antibodies targeting glycan-3 in hepatocellular carcinoma. *Sci Rep* 2016;6:33878.
  26. Wang X, Chang WC, Wong CW, et al. A transgene-encoded cell surface polypeptide for selection, in vivo tracking, and ablation of engineered cells. *Blood* 2011; 118:1255–1263.
  27. Li N, Fu H, Hewitt SM, et al. Therapeutically targeting glycan-2 via single-domain antibody-based chimeric antigen receptors and immunotoxins in neuroblastoma. *Proc Natl Acad Sci U S A* 2017;114:E6623–E6631.
  28. Maldarelli F, Wu X, Su L, et al. HIV latency. Specific HIV integration sites are linked to clonal expansion and persistence of infected cells. *Science* 2014;345:179–183.
  29. Ma C, Cheung AF, Chodon T, et al. Multifunctional T-cell analyses to study response and progression in adoptive cell transfer immunotherapy. *Cancer Discov* 2013;3:418–429.
  30. Donia M, Kjeldsen JW, Andersen R, et al. PD-1(+) polyfunctional T cells dominate the periphery after tumor-infiltrating lymphocyte therapy for cancer. *Clin Cancer Res* 2017;23:5779–5788.
  31. Rossi J, Paczkowski P, Shen YW, et al. Preinfusion polyfunctional anti-CD19 chimeric antigen receptor T cells are associated with clinical outcomes in NHL. *Blood* 2018;132:804–814.
  32. Miao HL, Pan ZJ, Lei CJ, et al. Knockdown of GPC3 inhibits the proliferation of Huh7 hepatocellular carcinoma cells through down-regulation of YAP. *J Cell Biochem* 2013;114:625–631.
  33. Siripongsakun S, Wei SH, Lin S, et al. Evaluation of alpha-fetoprotein in detecting hepatocellular carcinoma recurrence after radiofrequency ablation. *J Gastroenterol Hepatol* 2014;29:157–164.
  34. Martin-Padura I, Agliano A, Marighetti P, et al. Sex-related efficiency in NSG mouse engraftment. *Blood* 2010;116:2616–2617.
  35. Fisher B, Packard BS, Read EJ, et al. Tumor localization of adoptively transferred indium-111 labeled tumor infiltrating lymphocytes in patients with metastatic melanoma. *J Clin Oncol* 1989;7:250–261.
  36. Ishiguro T, Sugimoto M, Kinoshita Y, et al. Anti-glycan 3 antibody as a potential antitumor agent for human liver cancer. *Cancer Res* 2008;68:9832–9838.
  37. Ruiz de Galarreta M, Bresnahan E, Molina-Sanchez P, et al. Beta-catenin activation promotes immune escape and resistance to anti-PD-1 therapy in hepatocellular carcinoma. *Cancer Discov* 2019;9:1124–1141.
  38. Li J, Stagg NJ, Johnston J, et al. Membrane-proximal epitope facilitates efficient T cell synapse formation by Anti-FcRH5/CD3 and is a requirement for myeloma cell killing. *Cancer Cell* 2017;31:383–395.
  39. Haso W, Lee DW, Shah NN, et al. Anti-CD22-chimeric antigen receptors targeting B-cell precursor acute lymphoblastic leukemia. *Blood* 2013;121:1165–1174.
  40. Hou Y, Zou Q, Ge R, et al. The critical role of CD133(+) CD44(+/high) tumor cells in hematogenous metastasis of liver cancers. *Cell Res* 2012;22:259–272.
  41. Hamieh M, Dobrin A, Cabriolu A, et al. CAR T cell trogocytosis and cooperative killing regulate tumour antigen escape. *Nature* 2019;568:112–116.
  42. Faietta JA, Nobles CL, Sammons MA, et al. Disruption of TET2 promotes the therapeutic efficacy of CD19-targeted T cells. *Nature* 2018;558:307–312.
  43. Shah NN, Qin H, Yates B, et al. Clonal expansion of CAR T cells harboring lentivector integration in the CBL gene following anti-CD22 CAR T-cell therapy. *Blood Adv* 2019;3:2317–2322.
  44. Tang J, Li Y, Lyon K, et al. Cancer driver-passenger distinction via sporadic human and dog cancer comparison: a proof-of-principle study with colorectal cancer. *Oncogene* 2014;33:814–822.
  45. Yang CW, Hojer CD, Zhou M, et al. Regulation of T cell receptor signaling by DENND1B in TH2 cells and allergic disease. *Cell* 2016;164:141–155.

---

**Author names in bold designate shared co-first authorship.**

Received May 13, 2019. Accepted February 3, 2020.

#### Correspondence

Address correspondence to: Mitchell Ho, PhD, Laboratory of Molecular Biology, Center for Cancer Research, National Cancer Institute, National Institutes of Health, 37 Convent Drive, Room 5002, Bethesda, Maryland 20892-4264. e-mail: [homi@mail.nih.gov](mailto:homi@mail.nih.gov).

#### Acknowledgments

The authors thank Dr Steven Rosenberg (National Cancer Institute [NCI]) for valuable advice in the early stage of this study and for reading the manuscript. We thank the CCR LGI Flow Cytometry Core Facility in Building 37 for assistance of cell sorting. We also thank National Institutes of Health (NIH) Fellows Editorial Board, NIH Library Editing Service, Jessica Hong (NCI) and Bryan Fleming (NCI) for editorial assistance. The NCI holds patent rights to anti-GPC3 antibodies including YP7 and HN3 in many jurisdictions, including the United States (eg, US Patent 9409994, US Patent 9206257, US Patent 9394364, US Patent 9932406, US Patent Application 62/716169, US Patent Application 62/369861), China, Japan, South Korea, Singapore, and Europe. Claims cover the antibodies themselves as well as conjugates that utilize the antibodies, such as recombinant immunotoxins, antibody-drug conjugates, bispecific antibodies, and modified T-cell receptors/chimeric antigen receptors and vectors expressing these constructs. Anyone interested in licensing these antibodies can contact Mitchell Ho (NCI) for additional information.

#### CRediT Authorship Contributions

Dan Li, PhD (Conceptualization: Lead; Data curation: Lead; Formal analysis: Equal; Methodology: Equal; Writing – original draft: Equal; Writing – review & editing: Equal). Nan Li, PhD (Conceptualization: Equal; Data curation: Equal; Investigation: Lead; Methodology: Equal; Writing – original draft: Lead; Writing – review & editing: Equal). Yi-Fan Zhang, PhD (Data curation: Equal; Formal analysis: Supporting; Methodology: Equal). Haiying Fu, PhD (Data curation: Supporting; Formal analysis: Supporting; Methodology: Equal; Resources: Equal). Mingqian Feng, PhD (Conceptualization: Supporting; Data curation: Supporting; Methodology: Equal; Resources: Equal). Dina Schneider, PhD (Formal analysis: Supporting; Methodology: Equal; Resources: Equal). Ling Su,

PhD (Data curation: Equal; Methodology: Supporting; Resources: Equal). Xiaolin Wu, PhD (Conceptualization: Lead; Formal analysis: Equal; Methodology: Lead). Jing Zhou, PhD (Data curation: Lead; Formal analysis: Equal; Methodology: Lead; Resources: Supporting). Sean Mackay, PhD (Conceptualization: Equal; Formal analysis: Equal; Methodology: Lead; Resources: Equal). Josh Kramer, DVM (Data curation: Equal; Formal analysis: Supporting; Methodology: Equal; Resources: Supporting). Zhijian Duan, PhD (Data curation: Equal; Formal analysis: Equal; Resources: Supporting). Hongjia Yang, BS (Data curation: Supporting; Formal analysis: Supporting; Methodology: Equal; Resources: Supporting). Aarti Kolluri, BA (Data curation: Equal; Formal analysis: Supporting; Methodology: Equal). Alissa M. Hummer, BS (Data curation: Equal; Formal analysis: Supporting; Methodology: Equal; Resources: Supporting). Madeline B. Torres, MD (Formal analysis: Supporting; Methodology: Equal; Resources: Equal). Hu Zhu, PhD (Data curation: Equal; Formal analysis: Supporting; Methodology: Equal). Matthew D. Hall, PhD (Data curation: Equal; Formal analysis: Equal; Resources: Lead). Xiaoling Luo, PhD (Data curation: Equal; Methodology: Supporting; Resources: Equal). Jinqui Chen, PhD (Formal analysis: Equal; Methodology: Equal; Resources: Lead). Qun Wang, PhD (Formal analysis: Equal; Funding acquisition: Equal; Resources: Lead). Daniel Abate-Daga, PhD (Conceptualization: Equal; Formal analysis: Supporting; Resources: Equal). Boro Dropulic, PhD (Data curation: Lead; Methodology: Equal; Resources: Lead; Supervision: Equal). Stephen M. Hewitt, MD (Data curation: Equal; Formal analysis: Equal; Resources: Equal;

Validation: Lead). Rimas J. Orentas, PhD (Conceptualization: Equal; Formal analysis: Supporting; Methodology: Equal). Tim F. Greten, MD (Conceptualization: Lead; Data curation: Equal; Formal analysis: Equal; Investigation: Equal; Writing – review & editing: Equal). Mitchell Ho, PhD (Conceptualization: Lead; Formal analysis: Lead; Investigation: Lead; Methodology: Lead; Project administration: Lead; Supervision: Lead; Writing – original draft: Lead; Writing – review & editing: Lead).

#### Conflicts of interest

The authors disclose no conflicts.

#### Funding

This work was supported by the Intramural Research Program of NIH, NCI (Z01 BC010891 and ZIA BC010891) to MH. DL was a recipient of a predoctoral fellowship from the China Scholarship Council and supported by the Center for Cancer Research at the NCI and the NIH Graduate Partnerships Program in Bethesda, Maryland. HF was a recipient of a visiting fellowship from the China Scholarship Council. AK is a predoctoral fellow supported by the Mayo Clinic in Rochester, Minnesota (Clinical and Translational Science award UL1 TR000135), the Center for Cancer Research at the NCI and the NIH Graduate Partnership Program. The Leidos Biomedical Research, Inc in Frederick, Maryland was in part supported with federal funds from the NCI, NIH, under contract no. HHSN261200800001E.

## Supplementary Methods

### Cell Culture

The Hep3B (HCC), HepG2 (hepatoblastoma), A431 (epidermal carcinoma), and HEK-293T cell lines were purchased from American Type Culture Collection (Manassas, VA). G1 is a transfected A431 cell line stably expressing human GPC3.<sup>1</sup> Hep3B and HepG2 were transduced with lentiviruses expressing Luc. The Luc-expressing Huh-7 cell line was kindly provided by Dr Andras Heczey at Baylor College of Medicine (Houston, TX). The aforementioned cell lines were cultured in Dulbecco's modified Eagle medium supplemented with 10% fetal bovine serum, 1% L-glutamine, and 1% penicillin-streptomycin at 37°C in a humidified atmosphere with 5% CO<sub>2</sub>. Peripheral blood mononuclear cells from peripheral blood of healthy donors were isolated using Ficoll (GE Healthcare, Chicago, IL) according to the manufacturer's instructions. Peripheral blood mononuclear cells from HCC patients were isolated from peripheral blood after patients provided informed consent ([ClinicalTrials.gov](#) ID: NCT01313442). Jurkat T cells were purchased from ATCC. These cells were grown in RPMI-1640 medium supplemented with 10% fetal bovine serum, 1% L-glutamine, and 1% penicillin-streptomycin at 37°C in a humidified atmosphere with 5% CO<sub>2</sub>.

### Immunohistochemistry

The human HCC tissue and normal tissue microarrays were purchased from US Biomax (Rockville, MD). Tissue sections were deparaffinized with xylene and rehydrated in decreasing concentrations of ethanol. After antigen retrieval, endogenous peroxidase activity was inactivated in 3% hydrogen peroxide solution. The sections were blocked by 3% bovine serum albumin, then incubated with 1 µg/mL of the anti-GPC3 antibody YP7 for 2 hours at room temperature. After rinsing with Tris-HCl/0.05% Tween-20 buffer, sections were incubated at room temperature for 30 minutes with horseradish peroxidase-conjugated goat anti-mouse antibody. 3,3'-Diaminobenzidine reactions were performed after washes in Tris-HCl/0.05% Tween-20 buffer. Sections were counterstained with hematoxylin for 1 minute, dehydrated, and mounted with Permount mounting medium.

### Production of Glycan 3-Targeted Chimeric Antigen Receptor T cells

Recombinant GPC3-CAR lentiviral vectors were produced by co-transfecting with packaging plasmid psPAX2 and enveloping plasmid pMD2.G into HEK-293T cells using Calfectin (SigmaGen, Rockville, MD). Both psPAX2 and pMD2.G plasmids were gifts from Dr Didier Trono (Addgene #12260 and #12259). Lentiviral particles were collected from supernatant after 72 hours post-transfection and concentrated 100-fold by Lenti-X concentrator (Clontech, Mountain View, CA) in

accordance with manufacturer's instructions. Peripheral blood mononuclear cells from either healthy donors or HCC patients were stimulated for 24 hours using anti-CD3/anti-CD28 antibody-coated beads (Invitrogen, Carlsbad, CA) at a bead to cell ratio of 2:1 according to manufacturer's instructions in the presence of interleukin (IL) 2. To track T-cell numbers over time, viable cells were counted using trypan blue.

### Flow Cytometry

The cell surface expression of GPC3 on cells was detected by the anti-GPC3 mouse monoclonal antibody YP7 and goat-anti-mouse IgG-phycoerythrin (PE)-conjugated antibody (Jackson ImmunoResearch, West Grove, PA). The average number of GPC3 sites per cell was measured by using BD Quantibrite PE beads (BD Biosciences, San Jose, CA) according to the manufacturer's instructions. The transduction efficiencies of GPC3 CARs on T cells were detected by anti-EGFR human monoclonal antibody cetuximab (Erbitux) and goat-anti-human IgG-PE or allophycocyanin-conjugated antibody (Jackson ImmunoResearch). The CAR expression on Jurkat T cells was measured using GPC3-hFc fusion protein and goat-anti-human IgG-PE-conjugated antibody. The PE-conjugated anti-CD3, anti-CD4, and anti-CD8 antibodies were obtained from eBioscience (San Diego, CA). Data acquisition was performed using FACSCanto II (BD Biosciences) and analyzed using FlowJo software (TreeStar, Ashland, OR).

### Cytolytic Assay

The cytolytic activity of T cells transduced with GPC3-specific CARs was determined by a luciferase-based assay as described previously.<sup>2</sup> Briefly, CAR T cells and luciferase-expressing GPC3-positive (G1, Hep3B, HepG2, and Huh-7) and GPC3-negative (GPC3 knockout Hep3B, A431) tumor cells were incubated for 24 hours at different effector to target ratios. The luciferase activity was measured using the luciferase assay system (Promega, Madison, WI) on Victor (PerkinElmer).

Cytotoxicity of the CAR-expressing T cells was also tested by using the IncuCyte ZOOM system (Essen BioScience, Ann Arbor, MI). Briefly, T cells were added into GFP-expressing HepG2 tumor cells at effector to target ratio of 2:1. Images were taken every 2 hours up to 140 hours. The number of live cells was quantified based on the percentage of confluence of green fluorescence signals from target cells. The cell lysing activity was analyzed using the IncuCyte ZOOM liver cell imaging system.

### T-Cell Polyfunctionality Evaluation by Single-Cell Cytokine Profiling

Viable CAR T cells were enriched using Ficoll. CD4<sup>+</sup>/CD8<sup>+</sup> T-cell subsets were separated using anti-CD4 or anti-CD8 microbeads (Miltenyi Biotec, Bergisch Gladbach,

Germany) and stimulated with Hep3B, GPC3 knockout Hep3B, GPC3 overexpressing-A431 (G1) or GPC3-negative A431 cells at a ratio of 1:2 for 20 hours. A single cell functional profile was determined as described previously.<sup>3,4</sup> The PSI of each sample was computed using a prespecified formula,<sup>3</sup> defined as the percentage of poly-functional cells, multiplied by mean fluorescence intensity of the proteins secreted by those cells.

### Luminex Assay

Cytokine levels in supernatant collected after 24 hours of coculture of T cells and tumor cells were analyzed using the human cytokine 22-plex panel (granzyme B, GM-CSF, interferon gamma, TNF- $\alpha$ , IL-1 $\beta$ , IL-2, IL-4, IL-5, IL-6, IL-7, IL-10, IL-12, IL-13, IL-15, IL-21, CCL-3, CCL-4, CCL-19, CCL-20, CX3CL1, CXCL-11, and CXCL-8) on the Luminex system (Thermo Fisher Scientific, Waltham, MA).

### Western Blotting

For in vitro studies, cells were lysed with ice-cold lysis buffer (Cell Signaling Technology, Danvers, MA), and clarified by centrifugation at 10,000g for 10 minutes at 4°C. For tumors from in vivo studies, tissues were homogenized using the Bullet Blender according to manufacturer's instructions. Protein concentration was measured using a Bicinchoninic acid assay (Pierce, Rockford, IL) following the manufacturer's specifications. Twenty micrograms of cell lysates were loaded onto a 4%-20% sodium dodecyl sulfate polyacrylamide gel electrophoresis gel for electrophoresis. The anti-GPC3 antibody YP7 was developed in our laboratory. The anti-active- $\beta$ -catenin antibody was obtained from Millipore (Billerica, MA). All other antibodies were obtained from Cell Signaling Technology.

### $\alpha$ -Fetoprotein Assay

Serum  $\alpha$ -fetoprotein assay levels were determined using an enzyme-linked immunosorbent assay (GenWay Biotech, San Diego, CA) according to the manufacturer's instructions.

### Isolation of Immune Cells and Ex Vivo Analysis

At the time of animal sacrifice, cells were collected for flow cytometry or ex vivo analysis. Dissociation of tumor, liver, and spleen tissues was performed using Miltenyi Biotec tumor dissociation kit. Isolated T cells from these tissues were then stained for CD3, CD4, CD8, and CAR expression.

CD4 $^{+}$  or CD8 $^{+}$  T cells were recovered from spleens of the adoptive host and were separated with magnetic beads (Miltenyi Biotec). To analyze T-cell function, isolated T cells were cocultured with Hep3B cells, and the cytolytic activities were measured after 24 hours of coculture.

### Toxicologic Analysis

NSG mice from mock and CAR (hYP7) groups of the orthotopic Hep3B xenograft mouse model (healthy donor) were chosen for toxicology studies. Samples were processed for completed blood counts, comprehensive serum chemistry (VetScan, Abaxis Veterinary Diagnostics, Union City, CA) and internal organ weights. These analyses were performed by the Pathology/Histotechnology Laboratory in the National Cancer Institute (Frederick, MD).

### Droplet Digital Polymerase Chain Reaction

The primers and probe sequences are listed below.

Name	Sequence (5' to 3')
CAR-T vector	
Forward primer	GCAGTAGTCGCCGTGAAC
Reverse primer	TCACCAGGAGAAGCATGGTGG
Probe	56-FAM/AAGCTTACG/ZEN/CGTCCT AGCGCTAC/3IABkFQ
MLK2	
Forward primer	AGATCAGAAGGGTGAGAAAGAATG
Reverse primer	GGATGGTCTGGTAGTTGTAGTG
Probe	56-HEX/TGTTCCCTGC/ZEN/AACTGC AGATCCTGA/3IABkFQ

### Integration Site Analysis

The primers and probe sequences were listed in the below.

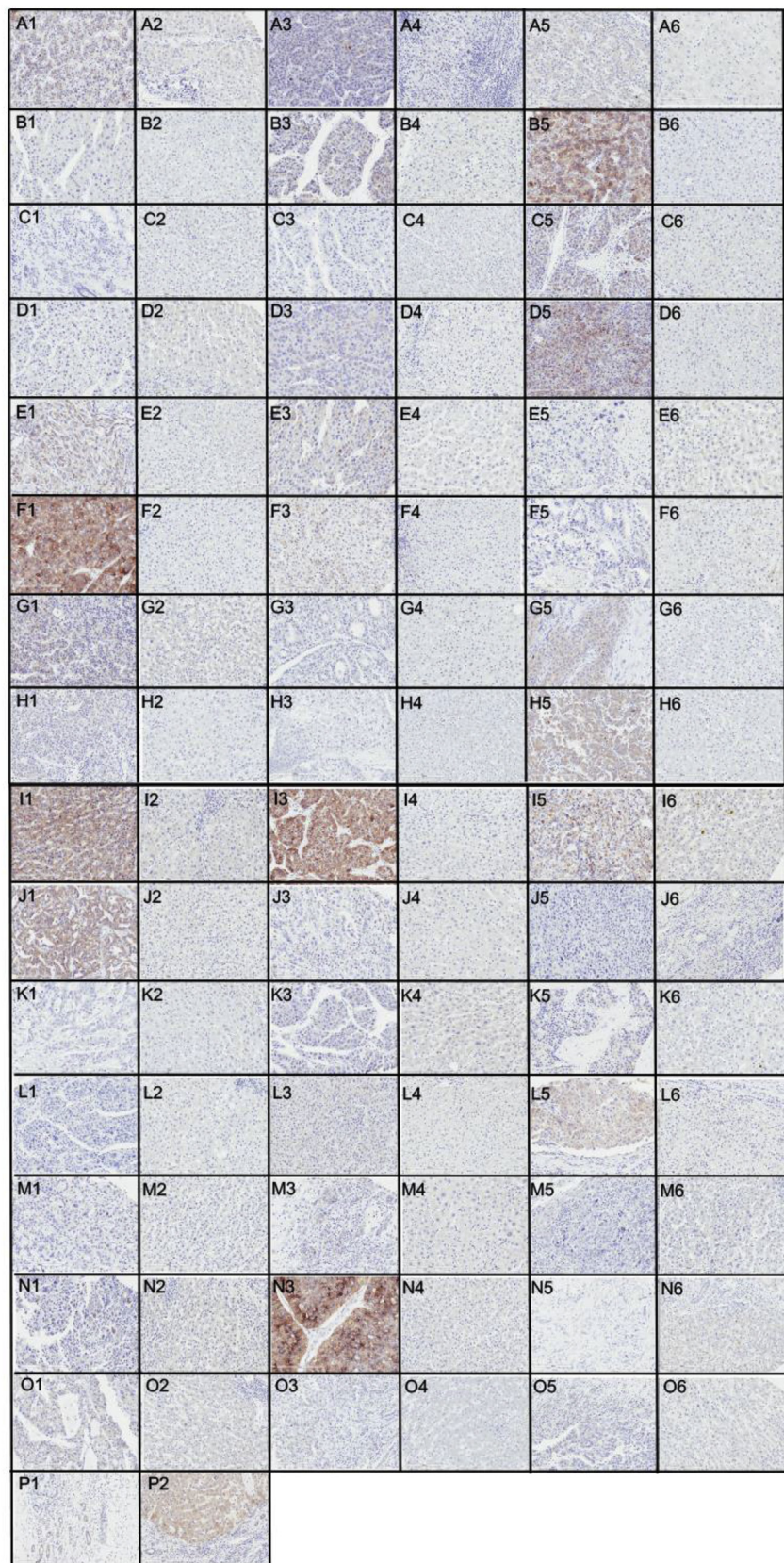
Name	Sequence (5' to 3')
First PCR	
3'LTR	CAAGATGGGATCAATTACCCA
Linker	GTAATACGACTCACTATAGGGC
Nest PCR	
3'LTR	CCCTTTAGTCAGTGTGGAAAATC
Linker	AGGGCTCCGCTTAAGGGAC

### Statistical Analysis

All experiments were repeated a minimum of 3 times. Data were analyzed and statistical analyses were performed using GraphPad Prism software (GraphPad, La Jolla, CA) and are presented as mean  $\pm$  SEM. Results were analyzed using unpaired Student *t* test (2-tailed). A *P* value of  $< .05$  was considered statistically significant. All statistical analyses were performed with Prism software.

### Supplementary References

1. Phung Y, Gao W, Man YG, et al. High-affinity monoclonal antibodies to cell surface tumor antigen glypican-3 generated through a combination of peptide immunization and flow cytometry screening. *MAbs* 2012;4:592–599.
2. Li N, Fu H, Hewitt SM, et al. Therapeutically targeting glypican-2 via single-domain antibody-based chimeric antigen receptors and immunotoxins in neuroblastoma. *Proc Natl Acad Sci U S A* 2017;114:E6623–E6631.
3. Ma C, Cheung AF, Chodon T, et al. Multifunctional T-cell analyses to study response and progression in adoptive cell transfer immunotherapy. *Cancer Discov* 2013;3:418–429.
4. Rossi J, Paczkowski P, Shen YW, et al. Preinfusion polyfunctional anti-CD19 chimeric antigen receptor T cells are associated with clinical outcomes in NHL. *Blood* 2018;132:804–814.
5. Gao H, Li K, Tu H, et al. Development of T cells redirected to glypican-3 for the treatment of hepatocellular carcinoma. *Clin Cancer Res* 2014;20:6418–6428.
6. Ishiguro T, Sugimoto M, Kinoshita Y, et al. Anti-glypican 3 antibody as a potential antitumor agent for human liver cancer. *Cancer Res* 2008;68:9832–9838.



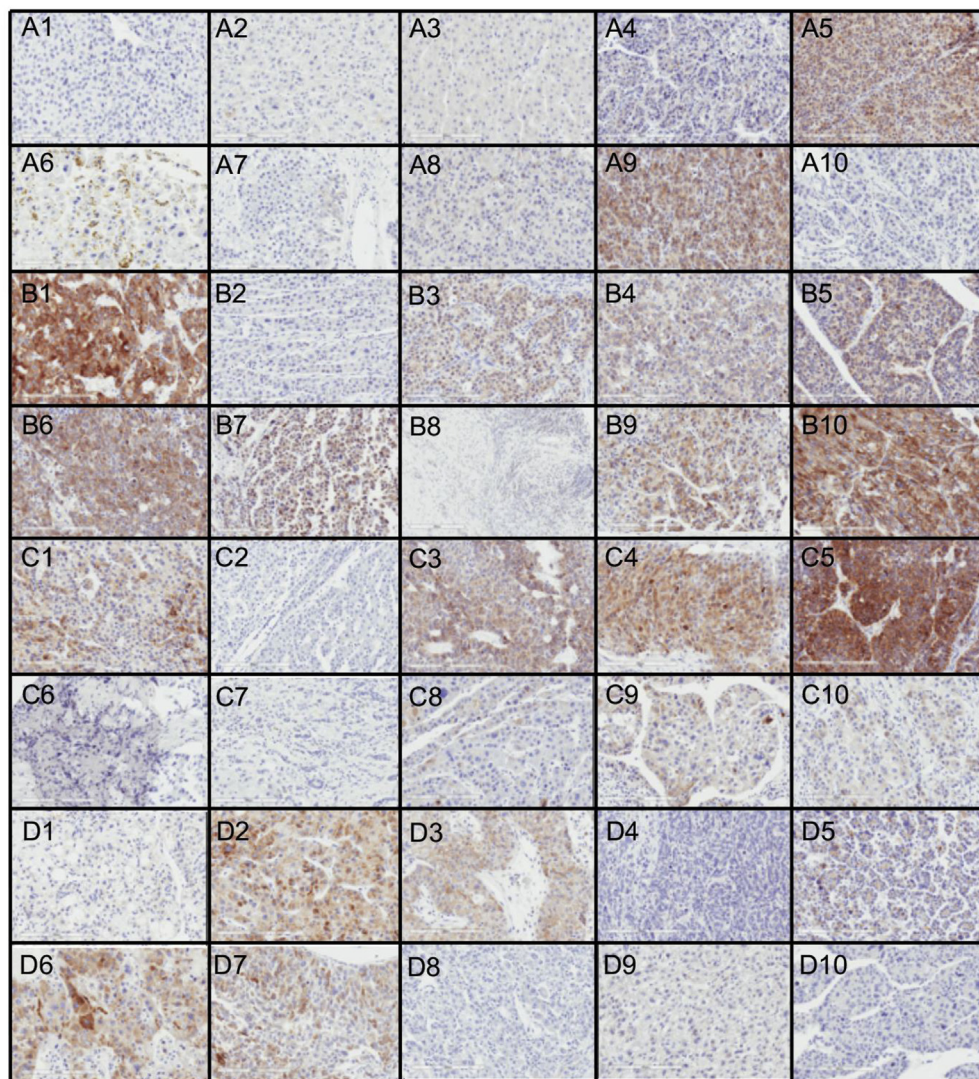
**Supplementary Figure 1.** GPC3 expression in HCC and paired adjacent normal liver tissues as determined by immunohistochemistry. GPC3 protein was highly expressed in 50% (23 of 46) of primary HCCs compared with only 2% (1 of 46) of matched tumor-adjacent tissues. The tissues were labeled with 1  $\mu$ g/mL YP7 antibody. The final magnification of all images was 200 $\times$ . Detailed information about each tissue specimen is listed. F, female; M, male; NAT, normal tissue adjacent to the tumor.

Position	Age, y	Sex	Organ/anatomic site	Pathology diagnosis	Grade	Type
A1	24	M	Liver	HCC	1	Malignant
A2	24	M	Liver	Hepatic cirrhosis	—	NAT
A3	52	M	Liver	HCC	2	Malignant
A4	52	M	Liver	Hepatitis	—	NAT
A5	66	M	Liver	HCC	1	Malignant
A6	66	M	Liver	Hepatic cirrhosis with fatty degeneration	—	NAT
B1	58	M	Liver	HCC	1	Malignant
B2	58	M	Liver	Hepatitis	—	NAT
B3	35	F	Liver	HCC	1	Malignant
B4	35	F	Liver	Hepatitis	—	NAT
B5	58	M	Liver	HCC	1	Malignant
B6	58	M	Liver	Cancer adjacent liver tissue	—	NAT
C1	56	M	Liver	HCC (sparse)	2	Malignant
C2	56	M	Liver	Hepatic cirrhosis	—	NAT
C3	41	M	Liver	HCC	2	Malignant
C4	41	M	Liver	Cancer adjacent liver tissue	—	NAT
C5	63	M	Liver	HCC	2	Malignant
C6	63	M	Liver	Hepatic cirrhosis	—	NAT
D1	48	F	Liver	HCC	2	Malignant
D2	48	F	Liver	Hepatic cirrhosis	—	NAT
D3	64	F	Liver	HCC	2	Malignant
D4	64	F	Liver	Hepatic cirrhosis	—	NAT
D5	53	F	Liver	HCC	2	Malignant
D6	53	F	Liver	Hepatic cirrhosis	—	NAT
E1	41	M	Liver	HCC	2	Malignant
E2	41	M	Liver	Hepatic cirrhosis	—	NAT
E3	45	M	Liver	HCC	1	Malignant
E4	45	M	Liver	Hepatic cirrhosis	—	NAT
E5	50	M	Liver	HCC	2	Malignant
E6	50	M	Liver	Hepatic cirrhosis with cholestasis	—	NAT
F1	51	F	Liver	HCC	2	Malignant
F2	51	F	Liver	Hepatitis	—	NAT
F3	63	M	Liver	HCC	2	Malignant
F4	63	M	Liver	Hepatitis	—	NAT
F5	63	F	Liver	HCC	2	Malignant
F6	63	F	Liver	Hepatic cirrhosis with cholestasis	—	NAT
G1	48	M	Liver	HCC	2	Malignant
G2	48	M	Liver	Hepatic cirrhosis	—	NAT
G3	67	M	Liver	HCC	2	Malignant
G4	67	M	Liver	Hepatic cirrhosis	—	NAT
G5	65	F	Liver	HCC	2	Malignant
G6	65	F	Liver	Hepatic cirrhosis	—	NAT
H1	58	F	Liver	HCC	2	Malignant
H2	58	F	Liver	Hepatic cirrhosis	—	NAT
H3	50	M	Liver	HCC	2	Malignant
H4	50	M	Liver	Hepatic cirrhosis	—	NAT
H5	61	M	Liver	HCC	3	Malignant
H6	61	M	Liver	Hepatic cirrhosis	—	NAT
I1	55	M	Liver	HCC	2	Malignant
I2	55	M	Liver	Hepatic cirrhosis	—	NAT
I3	60	M	Liver	HCC	2	Malignant
I4	60	M	Liver	Hepatic cirrhosis	—	NAT
I5	60	M	Liver	HCC	2	Malignant
I6	60	M	Liver	Hepatic cirrhosis with cholestasis	—	NAT
J1	58	M	Liver	HCC	2	Malignant
J2	58	M	Liver	Hepatic cirrhosis	—	NAT
J3	38	M	Liver	HCC	3	Malignant
J4	38	M	Liver	Hepatic cirrhosis	—	NAT
J5	69	M	Liver	HCC	2	Malignant
J6	69	M	Liver	Hepatic cirrhosis with cancer embolus	—	NAT
K1	61	F	Liver	(sparse)	—	NAT
K2	61	F	Liver	HCC	3	Malignant
K3	44	M	Liver	Hepatic cirrhosis	—	NAT
K4	44	M	Liver	HCC	2	Malignant
K5	43	M	Liver	Hepatic cirrhosis	—	NAT

Supplementary Figure 1. (continued).

K6	53	M	Liver	HCC	2	Malignant
L1	53	M	Liver	Hepatic cirrhosis	—	NAT
L2	41	F	Liver	HCC	2	Malignant
L3	41	F	Liver	Hepatitis	—	NAT
L4	62	M	Liver	HCC (sparse)	2	Malignant
L5	62	M	Liver	Hepatic cirrhosis	—	NAT
L6	47	M	Liver	HCC	2	Malignant
M1	47	M	Liver	Hepatitis	—	NAT
M2	56	F	Liver	HCC	3	Malignant
M3	56	F	Liver	Hepatic cirrhosis	—	NAT
M4	60	F	Liver	HCC	3	Malignant
M5	60	F	Liver	Hepatitis	—	NAT
M6	38	M	Liver	HCC	3	Malignant
N1	38	M	Liver	Hepatitis	—	NAT
N2	34	M	Liver	HCC	3	Malignant
N3	34	M	Liver	Hepatic cirrhosis	—	NAT
N4	54	F	Liver	HCC (sparse)	3	Malignant
N5				Hepatic cirrhosis with cholestasis	—	NAT
N6	32	M	Liver	HCC	3	Malignant
O1	32	M	Liver	Hepatic cirrhosis	—	NAT
O2	62	M	Liver	HCC	2	Malignant
O3	62	M	Liver	HCC	2	Malignant
O4				Hepatic cirrhosis with fatty degeneration	—	NAT
O5	58	M	Liver	HCC	3	Malignant
O6	58	M	Liver	Hepatic cirrhosis	—	NAT
P1	58	M	Liver	HCC	2	Malignant
P2	58	M	Liver	Hepatic cirrhosis	—	NAT

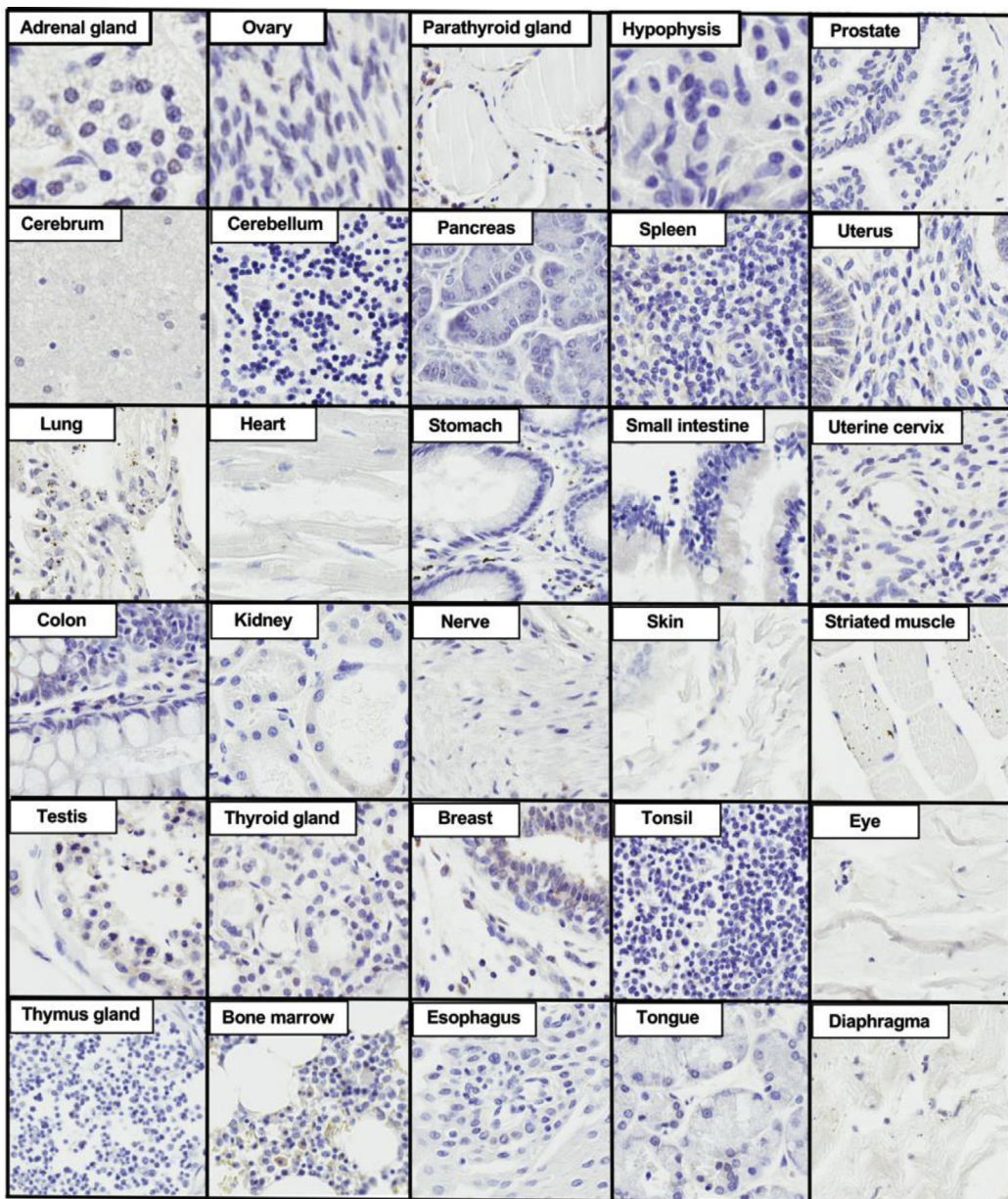
**Supplementary**  
**Figure 1. (continued).**

**Supplementary**

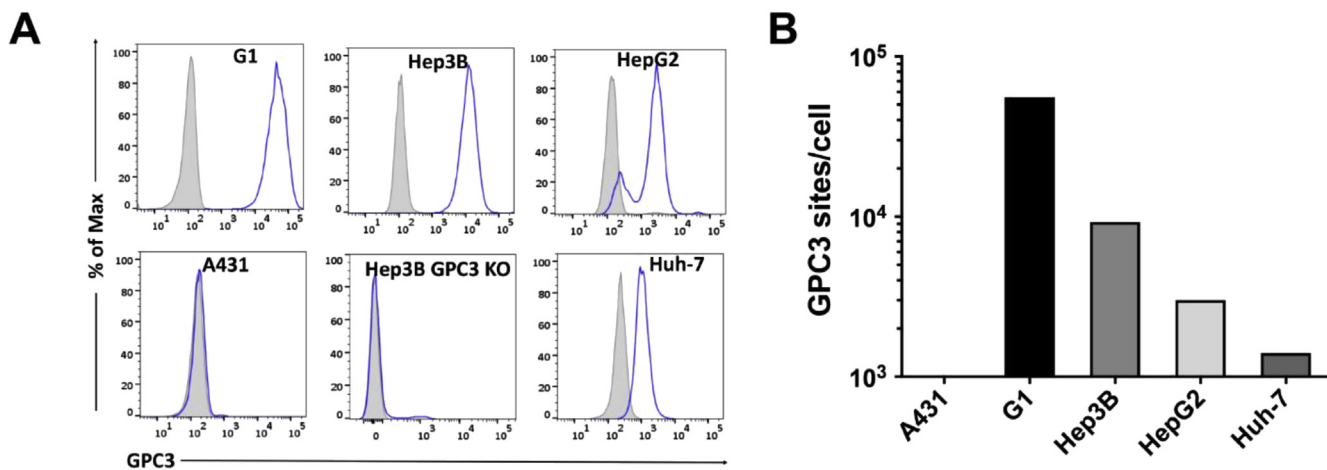
**Figure 2.** GPC3 expression in HCC tissues as determined by immunohistochemistry. Strong GPC3 staining was found in 60% (24 of 40) cases of HCC tissues. The tissues were labeled with 1  $\mu$ g/mL YP7 antibody. The final magnification of all images was 200 $\times$ . Detailed information about each tissue specimen is listed. F, female; M, male.

Position	Age, y	Sex	Organ/anatomic site	Pathology diagnosis	Grade	Type
A1	42	M	Liver	HCC	2	Malignant
A2	55	M	Liver	HCC	1	Malignant
A3	40	M	Liver	HCC	1	Malignant
A4	52	M	Liver	HCC	2	Malignant
A5	50	M	Liver	HCC	2	Malignant
A6	50	M	Liver	HCC	1	Malignant
A7	37	F	Liver	HCC	2	Malignant
A8	40	M	Liver	HCC	2	Malignant
A9	51	M	Liver	HCC	2	Malignant
A10	49	M	Liver	HCC	2	Malignant
B1	44	M	Liver	HCC	2	Malignant
B2	46	F	Liver	HCC	2	Malignant
B3	48	M	Liver	HCC	2	Malignant
B4	41	F	Liver	HCC	2	Malignant
B5	37	M	Liver	HCC	2	Malignant
B6	42	M	Liver	HCC	2	Malignant
B7	43	M	Liver	HCC	2	Malignant
B8	60	F	Liver	HCC	—	Malignant
B9	48	F	Liver	HCC	2	Malignant
B10	27	F	Liver	HCC	2	Malignant
C1	63	M	Liver	HCC	3	Malignant
C2	55	F	Liver	HCC	2	Malignant
C3	67	M	Liver	HCC	2	Malignant
C4	48	F	Liver	HCC	2	Malignant
C5	53	M	Liver	HCC	2	Malignant
C6	49	M	Liver	HCC	2	Malignant
C7	66	M	Liver	HCC	—	Malignant
C8	34	M	Liver	HCC	1	Malignant
C9	47	M	Liver	HCC	2	Malignant
C10	41	M	Liver	HCC	2	Malignant
D1	59	M	Liver	HCC	2	Malignant
D2	38	M	Liver	HCC	2	Malignant
D3	62	M	Liver	HCC	3	Malignant
D4	54	M	Liver	HCC	3	Malignant
D5	73	M	Liver	HCC	3	Malignant
D6	70	M	Liver	HCC	3	Malignant
D7	37	M	Liver	HCC	3	Malignant
D8	34	M	Liver	HCC	3	Malignant
D9	63	F	Liver	HCC	3	Malignant
D10	53	M	Liver	HCC	3	Malignant

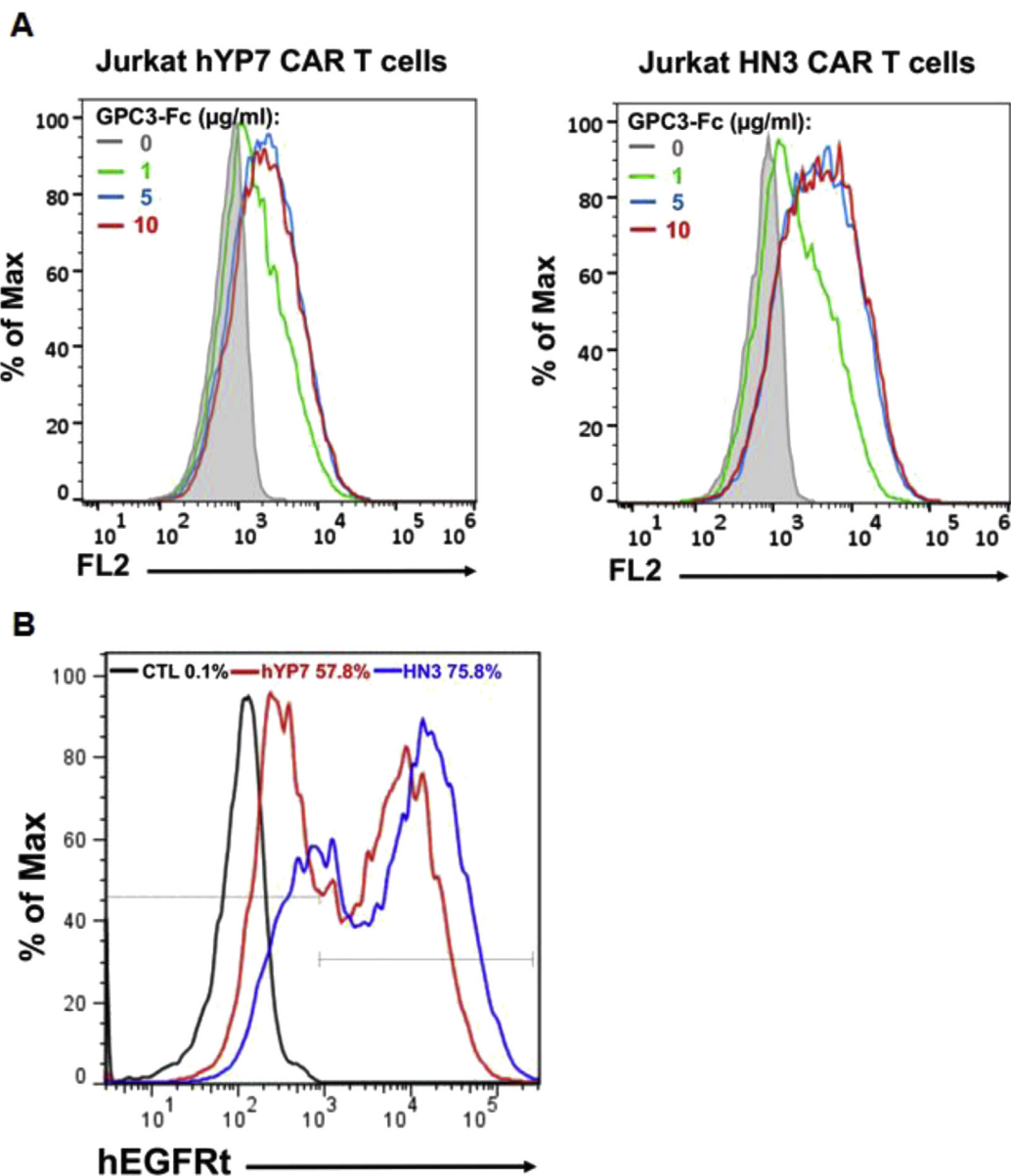
**Supplementary Figure 2. (continued).**



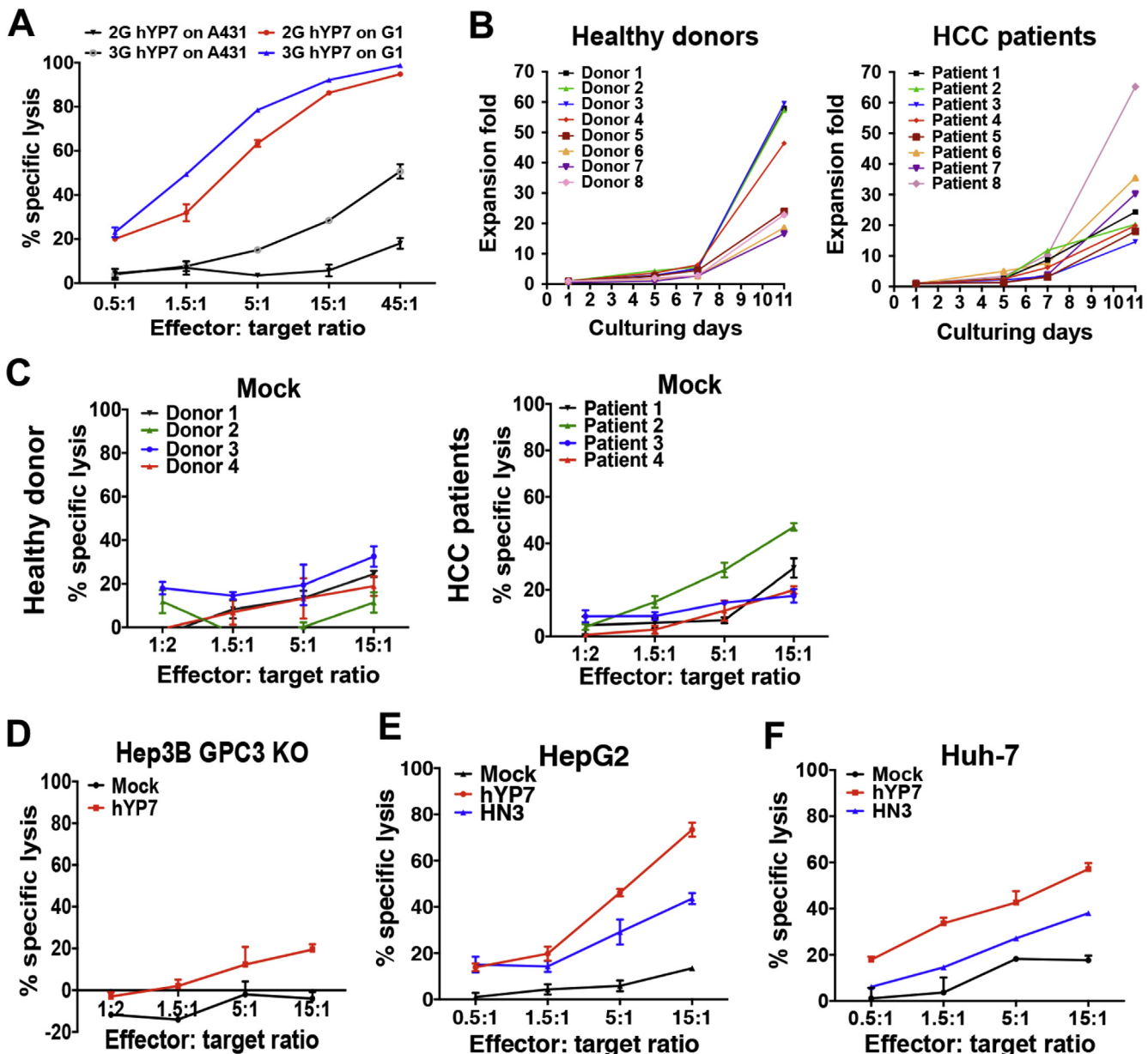
**Supplementary Figure 3.** Expression of GPC3 in 30 different human normal tissues as determined by immunohistochemistry. GPC3 protein was absent in normal tissues, including brain, heart, lung, stomach, small intestine, colon, kidney, pancreas, spleen, nerve, and skin. All tissues were stained with 1  $\mu$ g/mL YP7 antibody. The final magnification of all images was 200 $\times$ .



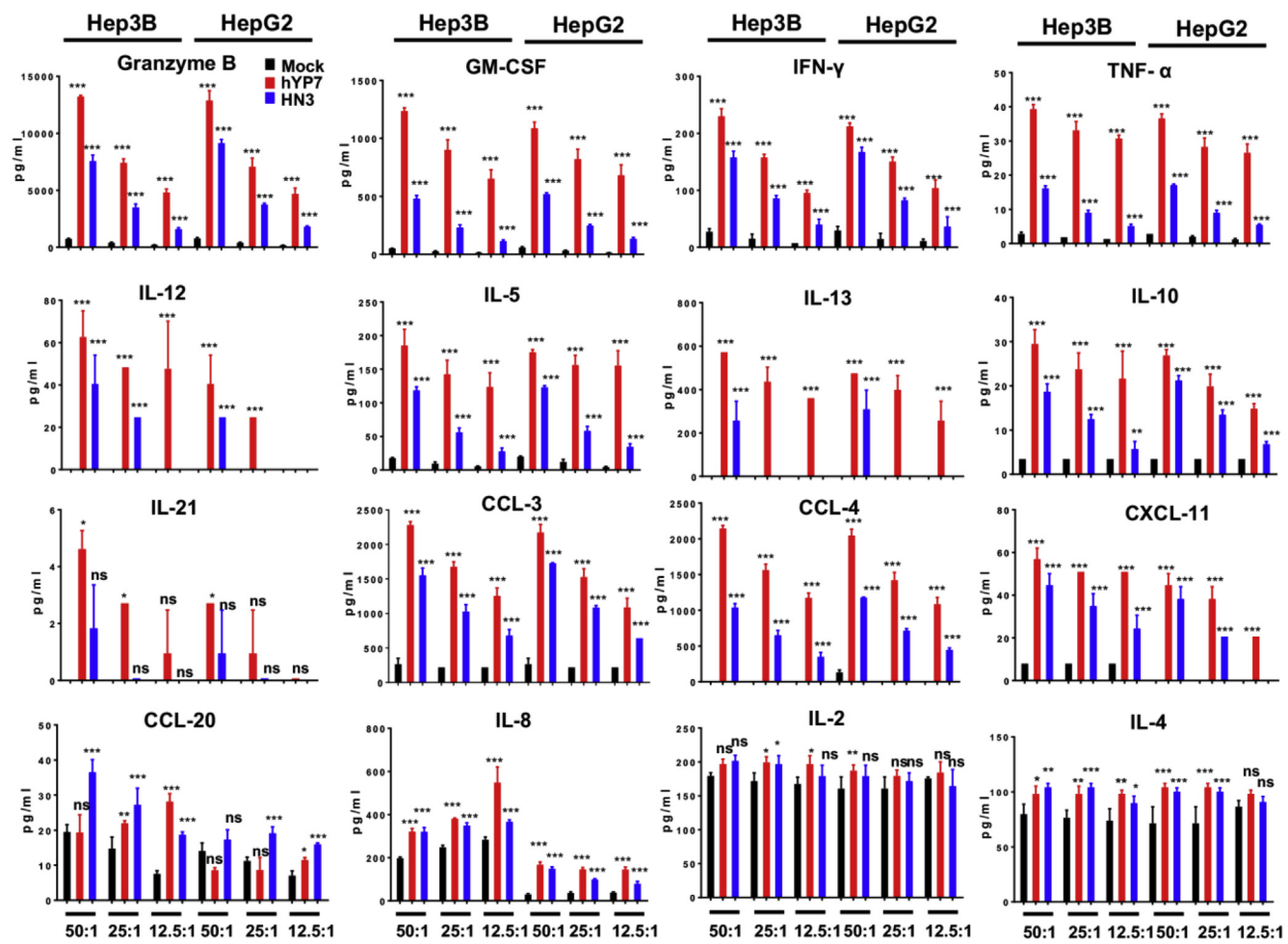
**Supplementary Figure 4.** GPC3 expression on cell surface as determined by flow cytometry. (A) YP7 exhibited specific binding to the GPC3-overexpressing A431 cells (G1) and liver cancer cell lines including Hep3B, HepG2, and Huh-7, but no binding to GPC3 knockout Hep3B cells and GPC3-negative cells (A431). *Shaded gray peaks* represent the cell surface staining with isotype control, *blue-colored peaks* represent the cell surface staining the YP7 antibody. (B) Quantification of GPC3 sites per cell using QuantiBrite PE beads.



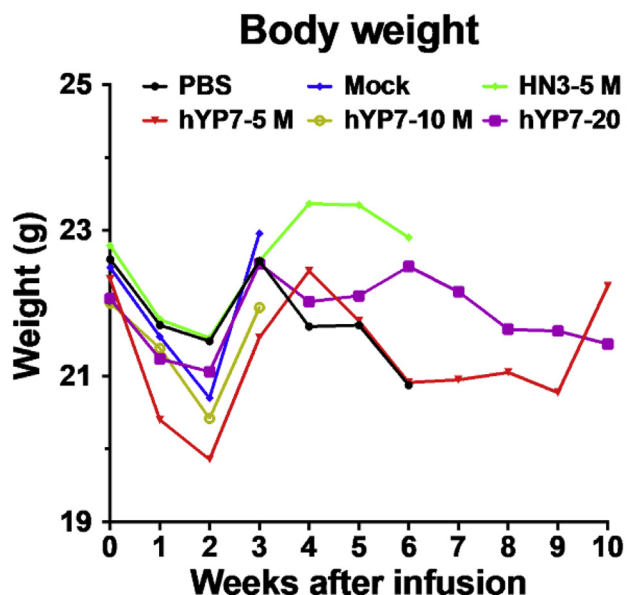
**Supplementary Figure 5.** Detection of GPC3-targeted CARs on cell surface by flow cytometry. (A) Expression of GPC3-targeted CARs in Jurkat T cells. Shaded gray peaks represent the cell surface staining with isotype control (CTL), and colorful solid line peaks represent the CAR expression on cell surface staining with different concentrations of GPC3-Fc protein. (B) CAR expression on T cells transduced with lentiviral particles was analyzed using flow cytometry by detection of truncated human epidermal growth factor receptor (hEGFRt) expression.



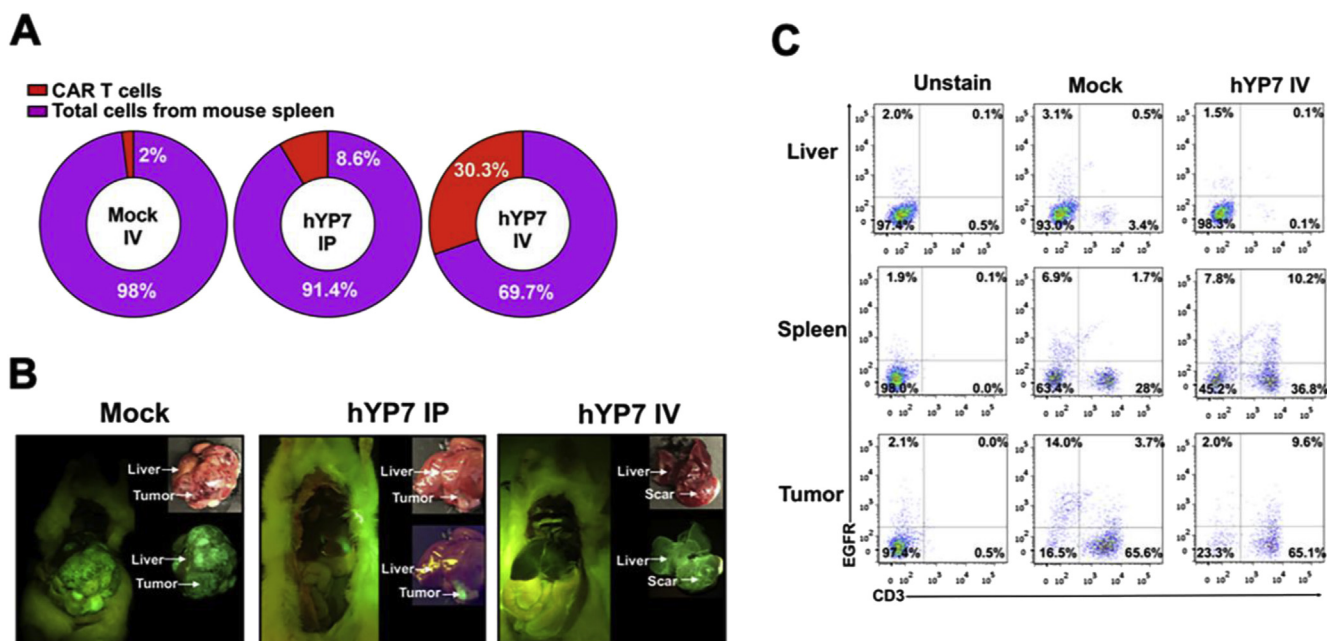
**Supplementary Figure 6.** Cytolytic activity and proliferation of GPC3-targeted CAR T cells in vitro. (A) Cytolytic activity of 2G CAR (hYP7) T cells and 3G CAR (hYP7) T cells after 24 hours of coculture with G1 (GPC3-overexpressing A431) and GPC3-negative A431 cells. (B) Proliferation of CAR (hYP7) T cells from healthy donors and HCC patients. (C) Minimal lysis of Hep3B cells by mock T cells from healthy donors and HCC patients. (D) No specific killing of GPC3 knockout Hep3B cells by CAR (hYP7) T cells after 24 hours of coculture. (E-F) Cytolytic activity of GPC3-specific CAR T cells after 24 hours of coculture with HepG2 and Huh-7 cells. Values represent mean  $\pm$  SEM.



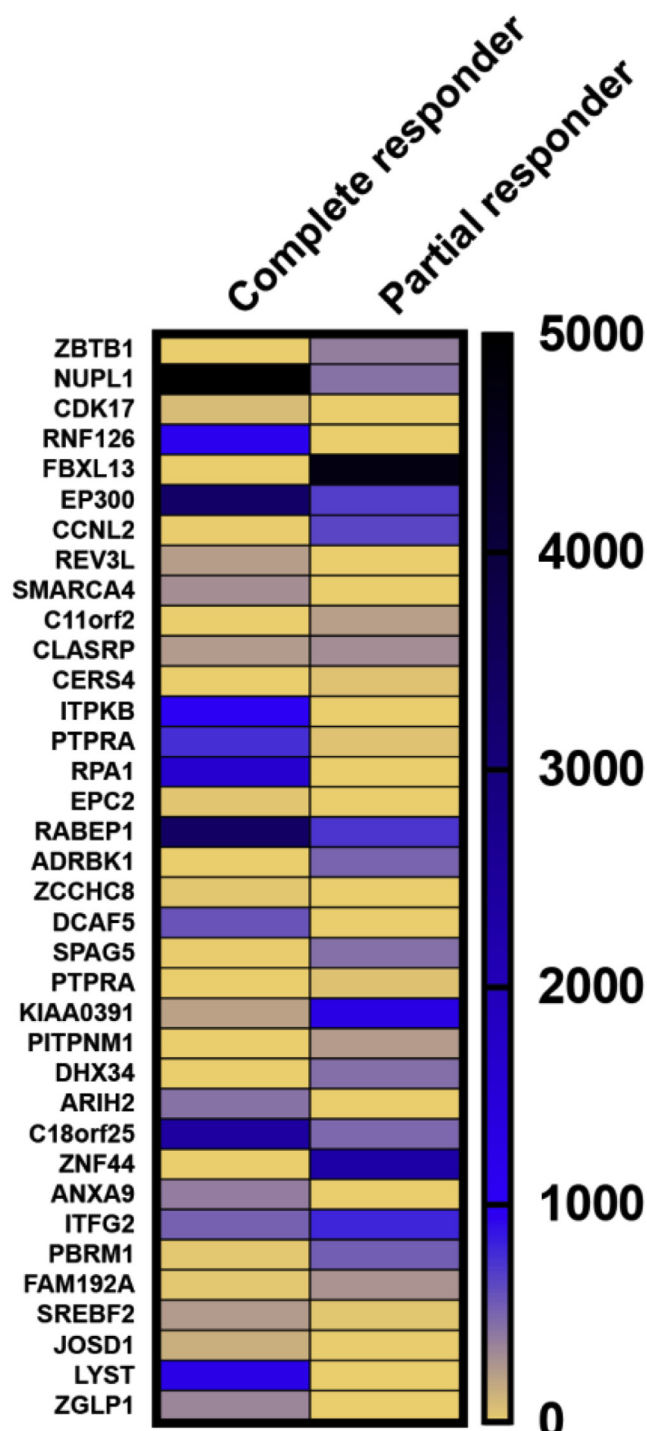
**Supplementary Figure 7.** Cytokine/chemokine profiles of T cells redirected with GPC3-targeted CARs. Hep3B or HepG2 cells were cocultured with GPC3-targeted CAR T cells for 24 hours at various effector to target ratios and indicated cytokine/chemokine levels in supernatants were measured using Luminex assay. Values represent mean  $\pm$  SEM. \* $P < .05$ ; \*\* $P < .01$ ; \*\*\* $P < .001$ ; ns, not significant.



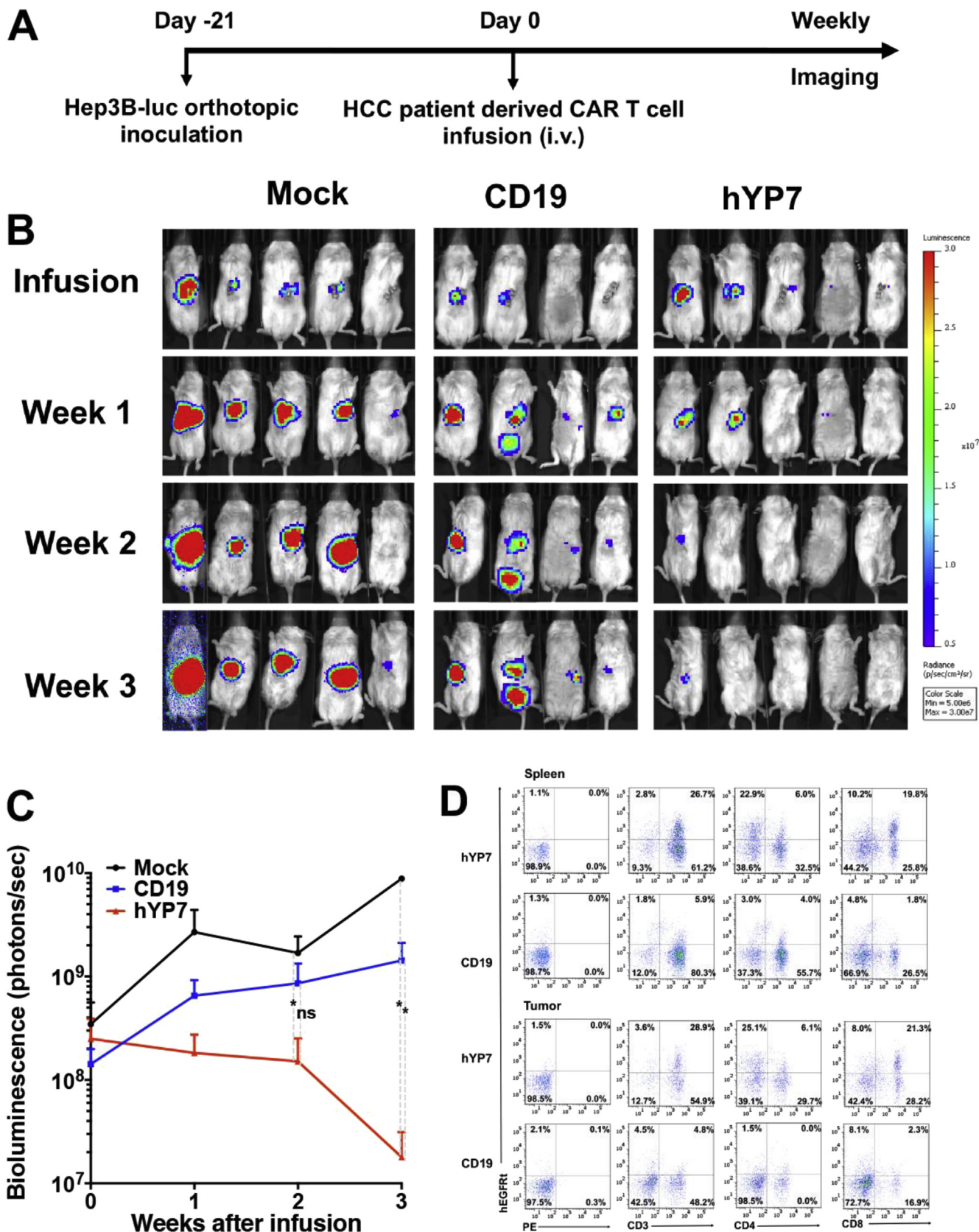
**Supplementary Figure 8.** Body weight of the peritoneal Hep3B tumor-bearing mice in different groups including phosphate-buffered saline (PBS) ( $n = 5$ ), mock T cells ( $n = 7$ ), HN3-5M ( $n = 8$ ), hYP7-5M ( $n = 7$ ), hYP7-10M ( $n = 5$ ), and hYP7-20M ( $n = 5$ ).



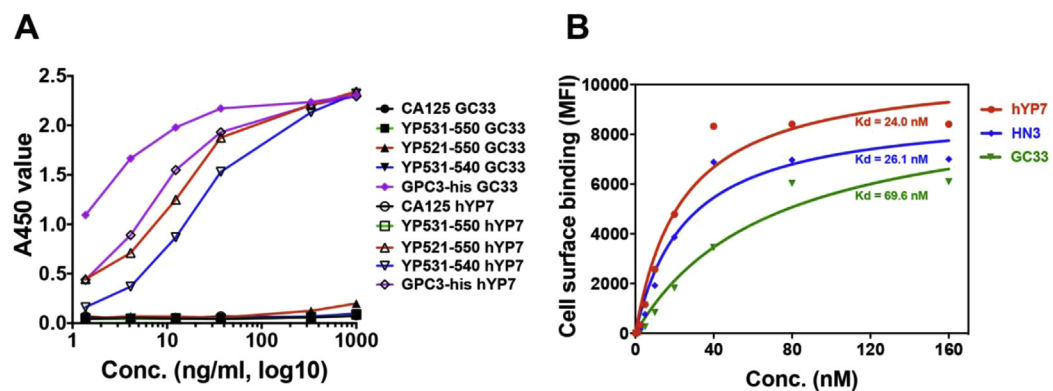
**Supplementary Figure 9.** Persistence of healthy donor derived-CAR (hYP7) T cells in the orthotopic Hep3B xenograft mouse model. (A) Existence of CAR vector-positive cells in mouse spleen after 7 weeks of administration as measured by ddPCR. (B) Representative pictures of mouse from mock, hYP7 IP and hYP7 IV groups at the end of study. (C) Evidence of CAR (hYP7) T cells in mice spleen and tumor microenvironment after 5 weeks of administration as determined by flow cytometry.



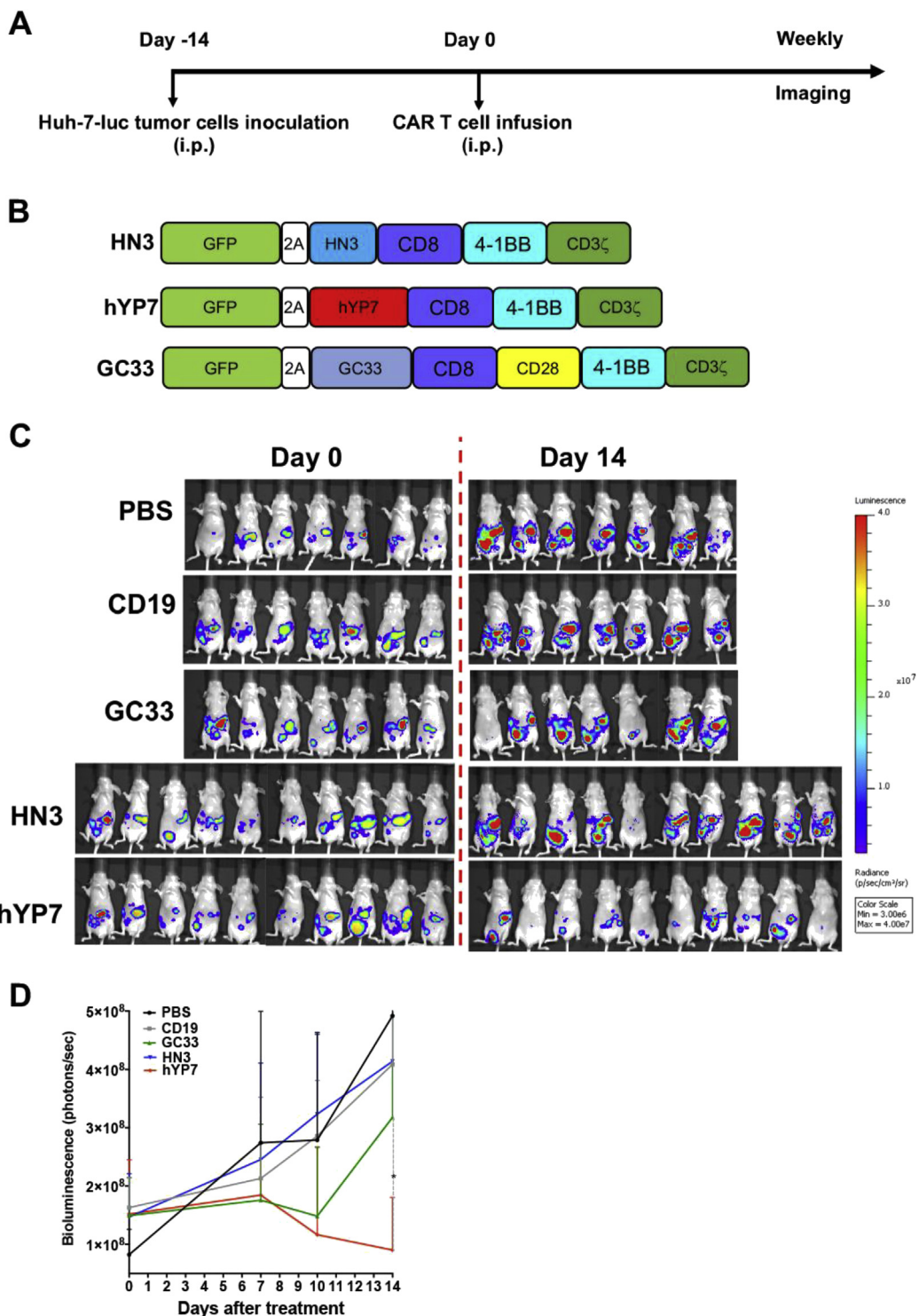
**Supplementary Figure 10.** The integration sites in a complete responder and a partial responder to healthy donor-derived CAR (hYP7) T-cell administration at week 7.



**Supplementary Figure 11.** Tumor eradication in the orthotopic Hep3B xenograft mouse model by CAR (hYP7) T cells from HCC patient no. 3. (A) Experimental schematic. NSG mice bearing orthotopic Hep3B tumors were IV injected with 5 million CD19 CAR T cells or CAR (hYP7) T cells. (B) CAR (hYP7) T cell administration regressed Hep3B tumor growth in mice. (C) Tumor bioluminescence in mice treated in panel B. (D) Analysis of CAR T-cell subpopulation in spleens and tumors from mice treated with CAR (hYP7) T cells or CD19 CAR T cells. Values represent mean  $\pm$  SEM. \* $P < .05$ ; \*\* $P < .01$ ; ns, not significant.



**Supplementary Figure 12.** The YP7 and GC33 monoclonal antibodies bind to GPC3 with distinct epitopes. The hYP7 antibody was used in this study. (A) Enzyme-linked immunosorbent assay analysis of binding of the hYP7 and GC33 to 3 GPC3 peptides. The hYP7 antibody is able to bind the YP521-540 and YP521-550 peptides, but not the YP531-550 peptide, whereas GC33 antibody shows no binding to any of these peptides. YP521-540 is the C-lobe fragment of GPC3 (amino acid 521–540): RFLAELAYDLDVDDAPGNSQ; YP521-550 is the C-lobe fragment of GPC3 (amino acid 521–550): RFLAE-LAYDLDVDDAPGNSQQATPKDNEIS; YP531-550 is the C-lobe fragment of GPC3 (amino acid 531–550): DVDDAPGNSQ-QATPKDNEIS. The GPC3-His protein is the full-length wild-type GPC3 (amino acid 25–550), and the CA125 is an irrelevant peptide control. (B) Flow cytometric analysis of hYP7, HN3 and GC33 binding affinities to GPC3 protein. The GPC3-targeted CARs including hYP7, HN3, and GC33 were expressed on Jurkat T cells.



**Supplementary Figure 13.** CAR (hYP7) T cells regress tumor growth in the peritoneal Huh-7 xenograft mouse model. (A) Experimental schematic. Huh-7 tumor-bearing nude mice were treated with intraperitoneal (i.p.) injection of phosphate-buffered saline (PBS), 10 million CD19 CAR T cells or 10 million GPC3-targeted CAR T cells. (B) Schematic diagram of GPC3-targeted CARs. The sequence encoding the HN3 or hYP7 antibody was cloned into a different lentiviral vector (Lentigen Technology, Inc, Gaithersburg, MD), which allows the expression of GFP and second-generation CAR. The previously reported 3G CAR<sup>5</sup> based on the anti-GPC3 antibody, GC33,<sup>6</sup> was included in this study. (C) CAR (hYP7) T cells demonstrated more potent antitumor activity than CAR (HN3) T cells or CAR (GC33) T cells after 2 weeks of injection. (D) Tumor bioluminescence in mice treated in panel C. Values represent mean  $\pm$  SEM. \* $P < .05$ .

**Supplementary Table 1.**The Clinical Information of Hepatocellular Carcinoma Patients

Patient no.	Age, y	Sex	Organ/anatomic	Treatment
1	60	Male	HCC	Tremelimumab
2	63	Male	HCC	Tremelimumab/TACE
<b>3</b>	<b>64</b>	<b>Male</b>	<b>HCC</b>	<b>Sorafenib</b>
4	59	Male	HCC	Screen tremelimumab
5	88	Male	HCC	Follow-up hepatectomy
6	57	Male	HCC	IVIG
7	65	Male	HCC	NA
8	78	Male	HCC	Duva/tremelimumab

IVIG, intravenous immunoglobulin; TACE, transarterial chemoembolization; NA, not available.

**Supplementary Table 2.**Toxicities of the Chimeric Antigen Receptor (Humanized YP7) T Cells From a Healthy Donor in the Orthotopic Hep3B Xenograft Mouse Model

Mouse group	Control	Control	Control	Control	hYP7 IP	hYP7 IV	hYP7 IV	hYP7 IV	hYP7 IV	Normal values
Mouse no.	807	426	427	428	765	793	772	530	535	—
Parameters										
White blood cells, K/ $\mu$ L	2.24	6.74	2.96	2.72	1.78	5.68	11.06	8.36	7.00	1.80–10.70
Red blood cells, M/ $\mu$ L	9.11	9.71	8.26	8.51	8.1	9.56	8.03	9.1	9.2	6.36–9.42
Neutrophils, K/ $\mu$ L	2.0	3.27	1.87	2.2	1.29	4.98	6.13	5.69	4.91	0.10–2.40
Albumin, g/dL	4.1	3.8	3.4	3.7	3.8	3.7	3.6	4.1	3.9	2.5–4.8
Alkaline phosphatase, U/L	70	60	70	70	41	73	88	142	82	62–209
Alanine aminotransferase, U/L	37	30	172	27	34	56	297	298	248	28–132
Total bilirubin, mg/dL	0.3	0.3	0.3	0.3	0.3	0.3	0.2	0.4	0.3	0.1–0.9
Creatinine, mg/dL	0.6	0.2	0.3	0.2	0.4	0.2	0.3	0.4	0.2	0.2–0.8
Globulin, g/dL	1.3	1.9	2.4	2.1	1.4	1	1.1	1.2	1.7	0.0–0.6
Total protein, g/dL	5.5	5.7	5.7	5.8	5.2	4.7	4.7	5.2	5.5	3.6–6.6
Blood urea nitrogen, mg/dL	14	14	18	16	18	28	23	21	18	18–29
Select organ weight, g										
Brain	0.497	0.449	0.408	0.461	0.519	0.459	0.46	0.476	0.509	—
Heart	0.106	0.152	0.11	0.133	0.138	0.088	0.102	0.112	0.132	—
Kidney	0.248	0.406	0.315	0.391	0.336	0.236	0.293	0.309	0.371	—
Liver	1.315	1.473	1.237	1.41	1.378	0.71	0.933	1.186	1.782	—
Lung	0.187	0.162	0.169	0.17	0.245	0.254	0.316	0.278	0.304	—
Spleen	0.041	0.046	0.055	0.461	0.119	0.035	0.055	0.075	0.106	—

NOTE. Mice receiving CAR (hYP7) T cells showed leukocytosis with an increased number of neutrophils, which were associated with a rapid immune response *in vivo*. Alanine aminotransferase activity was elevated, however, no gross evidence of liver damage was found at the post-mortem necropsy. All of the tested organ weights of the treated mice were similar to those of the control group, except for the lungs. No significant differences were detected in any other parameters measured.

**Supplementary Table 3.** The Shared Integration Sites in Spleens From Mice Treated With Healthy Donor-Derived Chimeric Antigen Receptor (Humanized YP7) T Cells After 5 Weeks

Gene	Integration site	Strand	Gene description
<i>NUPL1</i>	chr13: 25909144	-	Nucleoporin 58
<i>RABEP1</i>	chr17: 5234666	-	Rabaptin, RAB GTPase binding effector protein 1
<i>RNF126</i>	chr19: 649421	-	Ring finger protein 126
<i>C18orf25</i>	chr18: 43801810	+	Chromosome 18 open reading frame 25
<i>ZGLP1</i>	chr19: 10415946	+	Zinc finger GATA like protein 1
<i>CDK17</i>	chr12: 96830268	-	Cyclin dependent kinase 17
<i>REV3L</i>	chr6: 111707103	-	REV3 like, DNA directed polymerase zeta catalytic subunit
<i>CLASRP</i>	chr19: 45553045	+	CLK4 associating serine/arginine rich protein
<i>RPA1</i>	chr17: 1742043	-	Replication protein A1
<i>EPC2</i>	chr2: 149502287	-	Enhancer of polycomb homolog 2
<i>ZCCHC8</i>	chr12:122966998	-	Zinc finger CCHC-type containing 8

**Supplementary Table 4.** The Shared Integration Sites in Spleen and Tumor/Liver Tissues From Mice Receiving Hepatocellular Carcinoma Patient-Derived Chimeric Antigen Receptor (Humanized YP7) T Cells After 5 Weeks

Gene	Integration site	Strand	Gene description
<i>AP2A1</i>	chr19: 50297426	+	Adaptor related protein complex 2 subunit alpha 1
<i>CCNY</i>	chr10: 35628624	+	Cyclin Y
<i>RAB11FIP3</i>	chr16: 480813	+	RAB11 family interacting protein 3
<i>PIBF1</i>	chr13: 73362437	-	Progesterone immunomodulatory binding factor 1
<i>IL32</i>	chr16: 3127390	-	Interleukin 32
<i>C5orf42</i>	chr12: 90085625	+	Ciliogenesis and planar polarity effector 1
<i>LOC338758</i>	chr5: 37154931	-	ATP2B1 antisense RNA 1
<i>ZNF546</i>	chr19: 40506809	-	Zinc finger protein 546
<i>C1orf93</i>	chr1: 2511082	+	Peroxiredoxin like 2B
<i>TAPBPL</i>	chr12: 6564478	-	TAP binding protein like
<i>IKZF3</i>	chr17: 38018499	+	IKAROS family zinc finger 3
<i>ZZZ3</i>	chr1: 78051085	-	Zinc finger ZZ-type containing 3
<i>TMEM175</i>	chr4: 930834	-	Transmembrane protein 175
<i>DENND1B</i>	chr1: 197481279	+	DENN domain containing 1B
<i>EBF1</i>	chr5: 157858746	+	EBF transcription factor 1
<i>TLL5</i>	chr14: 76144276	+	Tubulin tyrosine ligase like 5
<i>MED25</i>	chr19: 50327804	-	Mediator complex subunit 25
<i>SLC25A44</i>	chr1: 156175971	-	Solute carrier family 25 member 44
<i>CBFB</i>	chr16: 67113306	-	Core-binding factor subunit beta
<i>INPP5K</i>	chr17: 1412114	-	Inositol polyphosphate-5-phosphatase K
<i>NDFIP2</i>	chr13: 80100317	-	Nedd4 family interacting protein 2
<i>TCEB3</i>	chr1: 24055329	+	Elongin A
<i>C19orf42</i>	chr19: 16752086	-	Small integral membrane protein 7